A ubiquitin-specific, proximity-based labeling approach for the identification of ubiquitin ligase substrates

Urbi Mukhopadyay[1,*], Sophie Levantovsky[2,*], Sarah Gharbi[1], Frank Stein[3], Christian Behrends[2,4], Sagar Bhogaraju[1,4]

Key words: ubiquitin, E3 ligase, substrate identification, BirA, RING, U box,

[1]European Molecular Biology Laboratory, 71 avenue des Martyrs, 38042, Grenoble, France
[2]Munich Cluster for Systems Neurology, Medical Faculty, Ludwig-Maximilians-Universität München, Munich, Germany
[3] Proteomics Core Facility, European Molecular Biology Laboratory, Heidelberg, Germany.
*These authors contributed equally to this work.

[4]Correspondence: Christian Behrends, Christian.Behrends@mail03.med.uni-muenchen.de; Sagar Bhogaraju, bhogaraju@embl.fr

Abstract:

Ubiquitination of proteins is central to protein homeostasis and other cellular processes including DNA repair, vesicular transport, cell-division etc. The process of ubiquitination is conserved from yeast to humans and is carried out by the sequential action of three enzymes: E1, E2 and E3. There are an estimated >600 E3 ligases in humans that execute ubiquitination of specific target proteins in a spatio-temporal manner to elicit desired signaling effects. Here, we developed a simple, proximity-based labeling method to selectively biotinylate substrates of a given ubiquitin ligase. Our method exploits the proximity and the relative orientation of the E3-ligase catalytic domain with respect to ubiquitin observed in the enzymatic intermediate-state structures of E3-E2~Ub. By fusing the biotin ligase BirA and an Avi tag variant to the candidate E3 ligase and ubiquitin, respectively, we were able to specifically enrich the *bona fide* substrates and potential new substrates of the ligase using a one-step Streptavidin pulldown under denaturing conditions. As proof-of-principle, we applied our method, which we named Ub-POD, to the RING E3 ligase Rad18. Rad18 ubiquitinates DNA-sliding clamp PCNA upon UV-induced DNA damage. We identified PCNA and several other critical players in the DNA damage repair pathway in a single Ub-POD experiment. We further discovered an unintended but important application of Ub-POD, where we were able to pin down the cellular localization of Rad18-mediated ubiquitination to the damaged DNA nuclear puncta through Streptavidin immunofluorescence. We also applied our method to TRAF6, another RING ubiquitin ligase involved in TNF signaling, successfully identifying known and potentially new substrates. Finally, we adapted our method to the U-box-type E3 ubiquitin ligase CHIP to demonstrate that we can identify substrates of two major classes of mammalian ubiquitin ligases. We anticipate that our method and principle could be widely adapted to all classes of ubiquitin ligases to identify substrates and localize the cellular site(s) of ubiquitination.

Introduction:

Similar to phosphorylation, ubiquitination of proteins has been found to have a role in virtually every cellular process in which it was investigated(*1*).Ubiquitination of substrates is achieved by three enzymes, E1, E2 and E3, acting in a cascade reaction and involves the covalent attachment of the terminal carboxyl group of Ubiquitin (Ub), a 76 amino acid long polypeptide, to substrate lysine through an isopeptide bond. The human genome encodes two E1's or Ub-activating enzymes, Uba1 and Uba6, that first adenylate the terminal carboxyl group of Ub using an ATP molecule, followed by the formation of a thioester linkage between Ub C-terminus and the catalytic cysteine of E1. There are ~40 E2's or Ub-conjugating enzymes which bind to E1 and catalyze a

transthioesterification reaction, resulting in an E2~Ub thioester conjugate. It is estimated that humans encode for >600 E3 ubiquitin ligases which confer specificity and functionality to the Ub cascade by targeted ubiquitination of thousands of cellular substrates(*1*). E3's bind the E2~Ub conjugate and the substrate to facilitate the transfer of Ub to target lysines of the substrate. The Really interesting new gene (RING) family of E3 ligases comprise the majority of E3's in the cell, with an estimated ~600 members(*2*). RING E3 ligases contain a conserved Zn^{2+}-binding RING domain and other auxiliary domains that bind E2~Ub and substrates, respectively. The RING domain spans ~70 residues and adopts a conserved alpha/beta topology. In RING E3-catalyzed ubiquitination, Ub is transferred directly from the catalytic cysteine of E2 to the substrate lysine residues. U-box E3 ligases also contain a RING-like catalytic domain that lacks the Zn^{2+}-binding site and operate as facilitators of ubiquitination, akin to the RING E3 ligases(*3*). Homologous to E6-AP carboxyl terminus (HECT) family comprises another major class of E3 ligase, with ~20 members in the human genome. HECT E3 ligases contain a conserved bi-lobal HECT domain at the C-terminus of the protein. The C-lobe of the HECT domain contains an invariant cysteine that accepts Ub from E2~Ub, before transferring the Ub to substrates. RBR (RING-between-RING) ligases possess two RING domains, one of which contains a catalytic cysteine that becomes transiently thioester linked to the Ub, prior to substrate ubiquitination(*4*).

Since E3 ligases are the concluding and decisive actors of all Ub signaling events; substrate identification of a given Ub ligase is critical for gaining insights into its cellular and physiological role. Traditional approaches of identifying protein-protein interactions, such as yeast two-hybrid and immuno-precipitation coupled proteomics, have provided valuable resources of potential substrates and the cellular pathways a given E3 ligase engages with(*5*). However, in most cases, E3-substrate interactions are transient and difficult to capture by these conventional methods. Many alternate methods have been developed to identify E3 ligase substrates and are reviewed here(*6*, *7*) in detail. A few such notable approaches are introduced here to provide context for the substrate identification method developed by us. One of the most powerful methods for the identification of E3 ligase substrates uses an antibody that specifically recognizes a diGly remnant that is characteristic of tryptic digested ubiquitinated substrates(*8*). Using quantitative comparison of diGly peptides from cells expressing wildtype (wt) or activity deficient mutant version of E3 ligases, one can identify the substrates and also the target lysines that are modified. Global protein stability (GPS) profiling uses the degradation profiles of the potential substrates fused to EGFP, coupled with the genetic perturbation of the E3 ligase to identify substrates(*9*, *10*). Another approach, UBAITS uses recombinant fusing of Ub to the E3 ligase of interest to covalently trap the ligase and its cognate substrates, as well as other interacting proteins(*11*). TULIP and TULIP2

103 methodologies build on the UBAITS principle and use HIS-tagged Ub-E3 ligase fusion, allowing
104 purification of the E3 ligase-substrate adduct in denaturing conditions(*12*, *13*). E2-dID uses biotin-
105 labeled Ub-E2 conjugates, plus wildtype or activity deficient mutant E3 ligase of interest, added
106 to the whole cell lysate *in vitro* to identify potential substrates(*14*). An orthogonal ubiquitin transfer
107 (OUT) approach has also been developed using engineered E1, E2 enzymes and E3 ligase of
108 interest that do not cross-react with the endogenous ubiquitin system, thus aiming to specifically
109 target the substrates of the engineered ubiquitin ligase of interest(*15*, *16*). Other notable methods
110 include using a microarray of purified human proteins in an *in vitro* assay(*17*) and a NEDDylator
111 approach, which uses Nedd8-E2 enzyme fused to the E3 ligase of interest(*18*). While no particular
112 method provides a silver bullet solution for the identification of E3 ligase substrates, each method
113 has been proven successful with a specific or a set of ligases and together these methods provide
114 an important toolbox in ubiquitin biology research.
115 Here we developed an approach to selectively and robustly label the substrates of a given E3
116 ubiquitin ligase directly in cells. Our approach relies on the conserved but transient intermediate
117 complexes that occur between E2~Ub and the E3 ligase in the case of RING E3 ligases and
118 E3~Ub that occurs during HECT E3 ligase-catalyzed ubiquitination. Based on the structural
119 information of E2~Ub-RING E3(*19*, *20*) complexes, we tagged the ligases of our interest with the
120 *E.coli* biotin ligase BirA enzyme and ubiquitin with an acceptor peptide (AP) tag. We co-
121 transfected these constructs in cells, resulting in the proximity & orientation-dependent tagging of
122 Ub (Ub-POD) during the BirA-E3-mediated ubiquitination, leading to biotin-labeled substrates. We
123 first tested this strategy using two unrelated human RING E3 ligases, Rad18 and TRAF6, which
124 are involved in UV-induced trans-lesion DNA synthesis and TNF signaling, respectively. We could
125 also localize the ubiquitination mediated by Rad18 precisely in cells using Ub-POD complemented
126 with Straptavidin immunofluorescence. Next, we successfully employed Ub-POD to a U-box
127 domain containing ligase, CHIP/STUB1 which is involved in the protein quality control machinery
128 by recognizing misfolded proteins and targeting them for degradation. Finally, we delineate the
129 principles and parameters of Ub-POD to facilitate other ubiquitin researchers to adopt Ub-POD
130 and identify the substrates of their favorite ligases.
131
132 **Results:**
133 **Concept of Ub-POD: a proximity and orientation-based labeling approach for identifying**
134 **E3 Ub ligase substrates**
135 During Ub transfer to the target proteins, RING E3 ligases bind both substrate and E2~ubiquitin
136 (E2~Ub) thioester conjugate, and mediate a direct transfer of ubiquitin from the E2 to the

137 substrate(*21*, *22*). Crystal structures of E2~Ub-RING E3 complexes have shown that RING E3s
138 first activate the E2~Ub thioester complex by forming a transient-intermediate complex between
139 E2~Ub and the RING E3 and subsequently orient the E2~Ub thioester complex with respect to
140 the substrate(*19*). In the UbcH5A~Ub-RNF4 complex structure reported by Plechanova *et al.*,
141 2012, we noted that the N terminus of the catalytic RING domain and N terminus of Ub point
142 towards the same orientation into solvent and come in close proximity to each other (~21 Å)
143 (Supplementary Figure 1A). Similarly, analysis of the HECT NEDD4L~Ub structures(*23*, *24*) has
144 revealed that the C-terminus of the HECT ligase, which harbors the catalytic HECT domain, and
145 the N-terminus of Ub orient towards each other into the solvent (Supplementary Figure 1B). These
146 observations prompted us to develop a precise ubiquitin-specific proximity based labeling
147 approach to identify the substrates of an E3 ubiquitin ligase. Proximity labeling approaches such
148 as BioID, TurboID and AirID have been used before to identify transient protein-protein
149 interactions(*25*–*27*). These methods depend on a mutated form of BirA or other engineered biotin
150 ligases fused to the protein of interest (POI) to release highly reactive AMP-Biotin into the
151 surrounding solvent and label the "neighboring" macromolecules with biotin. To develop a
152 proximity-based method specifically for the ubiquitination substrates, we tagged the catalytic end
153 of an E3 ubiquitin ligase using the wildtype *Escherichia coli (E.coli)* biotin ligase enzyme (BirA)
154 and the N-terminus of Ub with BirA's "acceptor peptide" (AP)(*28*) substrate (Figure1A). The
155 proximity and the orientation alignment between the E3 catalytic domain and the N-terminus of
156 Ub in the catalytic intermediate complex will enable BirA to catalyze site specific biotinylation of
157 AP linked to Ub. Subsequently, the biotinylated AP-Ub is transferred onto the target proteins,
158 allowing them to be efficiently isolated using Streptavidin immunoprecipitation (IP) and identified
159 through mass spectrometry (Figure1A-B). Unlike BioID, which uses BirA*, wildtype BirA does not
160 ligate biotin non-specifically to all the spatially proximal proteins but only attaches biotin to the
161 AP-Ub that is in close proximity to E3.
162
163 **Employing Ub-POD to identify substrates of the RING E3 ligase Rad18**
164 We first tested Ub-POD for substrate identification of the RING E3 ligase Rad18. Upon UV
165 induced bulky DNA lesions, Rad18, in a complex with the ubiquitin conjugating enzyme Rad6,
166 mediates monoubiquitination of proliferating cell nuclear antigen (PCNA), thereby triggering trans-
167 lesion synthesis of DNA(*29*). Since Rad18 contains the catalytic RING domain at the N-terminus,
168 we tagged the N-terminus of Rad18 with BirA to generate HA-BirA-Rad18 which we transiently
169 expressed along with AP-Ub in HEK-293 cells in the presence of biotin. After 24 hours, cells were
170 either exposed to UV or left untreated, followed by continued biotin treatment for 6 hours (Figure

171 1C, left panel, described in detail in the methods section). Cells were collected, lysed and the
172 whole cell lysates were subjected to SDS-PAGE, followed by immunoblotting with anti-
173 Streptavidin antibody. More biotinylation occurred in cells treated with UV relative to the non-
174 treated cells (Figure 1C, right panel), indicating that Ub-POD can monitor the activity of cellular
175 Rad18 retrospectively after lysis. Importantly, introduction of mutants (Rad18 C64D) disrupting
176 the interface of the Rad18-Rad6 complex resulted in loss of biotinylation, indicating that the BirA
177 tag on its own does not notably biotinylate AP-Ub other than in the context of catalysis-induced
178 proximity between BirA-Rad18 and AP-Ub (Figure 1C, right panel). Prompted by the positive
179 outcome of the immunoblotting experiment, we next employed proteomics to identify these
180 biotinylated proteins, which are the possible ubiquitination substrates of Rad18. We followed
181 similar experimental conditions as above and the biotinylated proteins were immunoprecipitated
182 (Iped) using Streptavidin beads under denaturing conditions from both UV treated and untreated
183 cells in triplicates (see methods). Quantitative mass spectrometry analysis of the Iped fraction
184 was performed using TMTplex labeling. We identified PCNA as the most enriched candidate
185 (Figure 1D, Supplementary table 1) in the UV-treated condition, providing us with a proof of
186 principle that the Ub-POD method can be employed to identify the substrates of a RING ubiquitin
187 ligase. Intriguingly, Melanoma associated antigen 4 (MAGEA4) was found enriched in the UV
188 untreated condition (Figure 1D, Supplementary table 1). MAGEA4 has been recently identified as
189 the stabilizer of Rad18 and was also shown to be ubiquitinated by Rad18 in *in vitro* ubiquitination
190 experiments(*30*). Our data indicates that Rad18 likely ubiquitinates MAGEA4 when cells are not
191 exposed to UV but preferentially ubiquitinates PCNA post UV-exposure of the cells. We further
192 sought to improve the specificity and sensitivity of substrate identification using Ub-POD to
193 increase the number of identified proteins and to improve the enrichment of substrates.
194
195 **A variant of AP tag improves the sensitivity of the Ub-POD method**
196 Due to a relatively high intrinsic affinity of AP for BirA, protein-protein interaction (PPI)
197 independent biotinylation may occur in cells, giving rise to background biotinylation of free AP-Ub
198 that is not primed for ubiquitination by the BirA tagged Ub ligase. Fernandez Suarez *et al.,* 2008
199 tested multiple variants of the AP sequences for their ability to specifically get biotinylated strictly
200 dependent on the proximity to the BirA labeled protein(*31*). Some of these variants included the
201 deletion of up to three amino acids from one or both ends of AP to decrease its interaction surface
202 area with BirA. Based on this, we prepared two variants of AP-Ub; (-2)AP-Ub in which two N-
203 terminal residues from the AP were removed and AP(-3) Ub in which C-terminal 3 residues of the
204 AP were removed (Figure 2A). In order to identify whether these truncated AP-Ub constructs can

205 increase the specificity and sensitivity of substrate detection, we overexpressed wildtype as well
206 as truncated AP-Ub constructs in HEK-293 cells, along with HA-BirA-Rad18, followed by biotin
207 treatment and UV exposure (Figure 2B). Streptavidin immunoblotting of the cell lysates showed
208 that in the presence of UV exposure, (-2) AP-Ub showed more biotinylation compared to wildtype
209 AP-Ub. AP(-3) Ub failed to show any notable biotinylation of possible targets (Figure 2B).
210 Therefore, we chose (-2)AP-Ub and used HA-BirA/(-2)AP-Ub as a control in our next proteomics
211 experiment. Upon incorporating these new measures, the overall number of identified hits
212 increased in the proteomics analysis compared to the experiment performed with AP-Ub (Figure
213 2C, 1D, Supplementary table 2). The gene ontology (GO) annotation analysis of the Ub-POD
214 Rad18 hits highlighted base excision repair, nucleotide excision repair and DNA replication
215 processes, which are highly relevant to the role of Rad18 in UV-induced DNA damage repair
216 (Figure 2C). Among the identified hits, DNA polymerase epsilon catalytic subunit (POLE) was of
217 particular interest to us, as this is a predicted substrate of Rad18 with a high confidence score in
218 Ubibrowser(*5*, *32*). POLE is crucial for optimal leading-strand DNA synthesis and POLE-mediated
219 leading-strand replication is dependent on the sliding-clamp processivity factor PCNA(*33*).
220 However, monoubiquitination of PCNA by Rad18 upon replication-stress results in the switching
221 of replicative polymerases (POLE and POLD) with trans-lesion synthesis polymerases. A previous
222 diGLY proteomics analysis aiming to identify DNA damage-induced ubiquitination events in
223 human cells revealed that ubiquitination of POLE is upregulated upon UV exposure of cells(*34*).
224 Identification of POLE as a hit in the Ub-POD experiment (Figure 2C) indicates that POLE might
225 be a substrate of Rad18.
226 The process of ubiquitination is reversible through the action of the deubiquitinase (DUB) family
227 of enzymes(*35*, *36*). This could potentially lead to the recycling of the biotinylated (-2)AP-Ub
228 employed in the Ub-POD experiment, potentially jeopardizing the specificity and efficiency of
229 substrate identification. To understand the impact of Ub recycling on the Ub-POD method, we
230 used a nonselective, broad spectrum DUB inhibitor PR-619 (2,6-diaminopyradine-3,5-
231 bis(thiocynate)) that efficiently silences four of the five DUB families(*37*). We treated the HA-BirA-
232 Rad18/ (-2)AP-Ub transfected cells with 10 uM of PR619, 2 hours post UV exposure. Proteomics
233 analysis showed that PR619 treatment increases the efficiency of PCNA identification compared
234 to non-treated cells (Figure 2D, Supplementary table 3). PR619 treatment also increased the
235 overall number of proteins identified as hits and GO annotation analysis showed that most of the
236 identified hits are related to the process of damaged DNA binding (Figure 2D). We identified
237 several proteins which are predicted to be RAD18 substrates by the repositories such as
238 Ubibrowser(*5*), BioGRID(*38*), Reactome(*39*) and these candidates have been highlighted in

239 supplementary table 3. Our data indicates that a pan DUB inhibitor treatment further improves
240 substrate identification by Ub-POD.
241 Identifying the substrate(s) of a give ubiquitin ligase is crucial to delineate its function. Additionally,
242 visualizing where in the cell the ubiquitination of substrates is taking place is also important as it
243 can add cellular context to understanding the function of the ligase. A Ub-POD experiment
244 complemented by Streptavidin immunofluorescence can in principle reveal the cellular
245 localization of ubiquitinated substrate. Rad18-mediated PCNA monoubiquitination and the
246 following polymerase switching event take place at the UV-irradiation induced Rad18 nuclear
247 foci(*40*). To test if Ub-POD can visualize PCNA ubiquitination at the nuclear damaged DNA foci,
248 we performed double immunostaining with Streptavidin (to detect the site of the biotinylation
249 event) and HA antibody (to detect Rad18). Remarkably, the Streptavidin signal was observed at
250 the nuclear puncta only in HA-BirA-Rad18 expressing cells and not in HA-BirA expressing cells
251 (Figure 2E-F). Moreover, Streptavidin and HA showed co-localization at these nuclear puncta
252 (Figure 2G), indicating that Ub-POD can indeed visualize the cellular localization of a given E3
253 ligase-mediated ubiquitination reaction.
254
255 **Employing Ub-POD on the RING E3 ligase, TNF receptor-associated factor 6 (TRAF6)**
256 We next sought to benchmark our approach with the well-studied RING E3 ligase, TRAF6 which
257 mediates K63 ubiquitin linkage types in concert with the ubiquitin-conjugating enzyme
258 heterodimer UBE2N-UBE2V1. TRAF6 bridges tumor necrosis factor (TNF) receptor activation via
259 exogenous agents or endogenous mediators and subsequent activation of transcriptional
260 responses via NF-κB and MAPK pathways(*41*, *42*).
261 We transiently co-transfected HEK-293 cells with (-2)AP-Ub and N-terminally tagged HA-BirA-
262 TRAF6 or HA-BirA for 24 h, and subsequently treated the cells with biotin for 15 min. To stimulate
263 TRAF6 dimerization and thereby activation, cells were additionally treated with TNF-α (Figure
264 3A). Analysis via immunoblotting confirmed the capability of HA-BirA-TRAF6 to biotinylate
265 potential substrate proteins in the presence of biotin, in contrast to expression of HA-BirA alone
266 (Figure 3B). Interestingly, downstream phosphorylation of NF-κB was already induced by HA-
267 BirA-TRAF6 overexpression alone, without TNF-α treatment (Figure 3B). Consistently,
268 biotinylation levels in HA-BirA-TRAF6 expressing cells are similar with or without TNF-α
269 treatment, indicating at least for the purpose of this Ub-POD experiment, HA-BirA-TRAF6
270 overexpression alone could be used to identify TRAF6 substrates.
271 We proceeded with these samples to the Streptavidin pulldown followed by on-beads tryptic
272 digestion and MS analysis. Across the different conditions, quadruplicate samples showed high

273 Pearson correlation (r ≥ 0.928). In total, we identified 2,145 proteins of which 1,331 proteins
274 passed our filtering criteria (See methods). 503 proteins were significantly enriched in HA-BirA-
275 TRAF6 expressing cells compared to HA-BirA control expressing cells. 231 of these proteins
276 reached the threshold of FDR <0.05 and fold change >1 (Figure 3C). GO annotation analysis of
277 proteins reaching the threshold FDR<0.05 and FC >1 (231 proteins) unveiled shared protein
278 motifs, such as E3 ligase domains (RING and HECT) and ubiquitin-interacting motifs (UIM).
279 Interestingly, positively regulated hits showed specific enrichment of proteins involved in immune
280 response pathways against bacterial and viral infection, including Toll-like receptor and NF-κB
281 signaling pathway, amongst others, which gives us confidence in the robustness of our approach
282 even in non-immune cell types such as HEK-293 cells (*42*, *43*) (Figure 3C, right panel).
283 TRAF6 is the strongest regulated hit due to its autoubiquitination in the active and oligomerized
284 state. Furthermore, our approach enabled the specific enrichment of bona fide TRAF6 substrates
285 (IKBKG, IRAK1, MAP3K7, HK2)(*42–45*) (Figure 3C, left panel, Supplementary table 4).
286 Interestingly, we also enriched for the deubiquitinating enzyme complex (BRISC), which is specific
287 for lysine 63-linked ubiquitin hydrolysis(*46*). Furthermore, strongly regulated hits are VHS-domain
288 containing and Ub-binding proteins located at endosomes (STAM, HGS, TOM1), which are
289 involved in receptor tyrosine kinase (RTK)-mediated endocytosis(*47*).
290 Similar results were obtained by statistical analysis of HA-BirA-TRAF6 treated with TNF-α versus
291 HA-BirA control, supporting the hypothesis that additional TNF-α stimulation does not result in an
292 increase in biotinylation of candidate substrates (Supplementary Figure 2A, Supplementary table
293 5). Comparing TNF-α treated versus mock treated HA-BirA-TRAF6 expressing cells does not
294 enrich for known TRAF6 targets and no significant hits reach significance with false-discovery
295 rate <0.05 (Supplementary Figure 2B, Supplementary table 6).
296

297 **Employing Ub-POD to identify substrates of U-box domain containing E3 Ubiquitin ligase,**
298 **CHIP/STUB1**

299 Next, we asked if Ub-POD can be applied to a U-box domain containing Ub ligase. The U-box
300 domain adopts the same fold as the RING domain but lacks the Zn^{2+} coordination residues which
301 are replaced by a tight hydrogen bonding network, contributing to the integrity of the catalytic
302 domain structure(*48*, *49*). CHIP (carboxyl terminus of Hsc70-interacting protein) which is also
303 called STUB1 (STIP1 homology and U box-containing protein 1) is a U-box domain containing Ub
304 ligase that functions as a key regulator of the protein quality control machinery. CHIP binds the
305 molecular chaperones Hsc70, Hsp70 and HSP90 through its N terminal tetratricopeptide repeat
306 (TPR) domain and facilitates the polyubiquitination of misfolded client proteins via its C-terminal

307 catalytic U-box(*50–52*). We employed Ub-POD on the CHIP ligase for benchmarking the
308 approach for a U-box E3 ligase and to possibly identify new substrates of CHIP. In line with the
309 concept of Ub-POD, we prepared a CHIP construct where BirA is tagged to the C-terminus of
310 CHIP (CHIP-BirA-HA), since the catalytic U-box domain of CHIP is located at the extreme C-
311 terminus of the protein (Figure 4A). We also designed another construct in which we inserted a
312 GSGS linker between the catalytic U-box domain of CHIP and BirA (CHIP-GSGS-BirA-HA)
313 (Figure 4A), under the assumption that providing more degrees of freedom for BirA improves BirA-
314 mediated site specific biotinylation of (-2)AP-Ub and thus leads to more efficient target protein
315 biotinylation. CHIP-BirA-HA or CHIP-GSGS-BirA-HA were transiently expressed in HEK-293
316 cells, along with (-2)AP-Ub. As CHIP directs target proteins for proteasomal degradation, we
317 treated cells with the proteasome inhibitor MG132 to preserve the substrates for the duration of
318 the experiment. Cells not treated with MG132 were taken as controls in our western blotting
319 experiments. Streptavidin immunoblotting showed that in presence of MG132, both CHIP-BirA-
320 HA and CHIP-GSGS-BirA-HA had enrichment of ubiquitinated substrates compared to the
321 MG132 untreated counterparts (Figure 4B). Interestingly, CHIP-GSGS-BirA-HA showed more
322 biotinylation compared to CHIP-BirA-HA, suggesting that the linker improves efficiency of
323 biotinylation of potential substrates, at least in the case of CHIP (Figure 4B). Since the structure
324 of CHIP in complex with E2 is known(*53*), we designed a mutant of CHIP (I235DF237D) that is
325 deficient in binding to E2 as a negative control (Figure 4A-B). As expected, the biotinylation is
326 notably lower in the condition where CHIP (I235DF237D)-BirA-HA is transfected compared to
327 wildtype CHIP-BirA-HA. We chose CHIP-GSGS-BirA-HA for the identification of potential
328 substrates through proteomics. We did not induce proteotoxicity in this experiment, since we
329 sought to identify substrates that get ubiquitinated by CHIP under basal conditions. Hypoxia
330 inducible transcription factor, HIF1A, a very well-known substrate of CHIP(*54*), was specifically
331 identified in conditions where CHIP-GSGS-BirA-HA is expressed (Figure 4C, supplementary table
332 7). In addition, CHIP is reported to tag proteasomal subunits with polyubiquitin chains and target
333 them to aggresomes(*55*). In agreement with this, several proteasomal subunit proteins were also
334 identified as hits in the proteomics analysis (supplementary table 7). Since CHIP is involved in
335 several different cellular processes apart from protein quality control(*56*), we wondered whether
336 we could identify additional substrates of CHIP by temporally controlling the exposure of biotin to
337 CHIP-GSGS-BirA-HA expressing cells. Therefore, instead of exposing the cells to biotin
338 immediately after transfection, we added biotin to cells 24h after the transfection, along with
339 MG132 (Supplementary Figure 3A). Interestingly, two other known substrates of CHIP, SQSTM1
340 (also known as p62)(*57*) and SOD2(*58*) were identified (Supplementary Figure 3B,

341 Supplementary table 8) with this short biotin exposure. This change in substrate identification
342 profile depending on the duration of biotin pulse could be due to the different half-lives of various
343 substrates of the CHIP Ub ligase. GO annotation analysis of hits identified in both biotin treatment
344 regimes, however, highlighted similar processes relevant to known functions of CHIP, such as
345 ubiquitin-mediated proteolysis, pathways of neurodegeneration, and protein processing in the
346 endoplasmic reticulum (Figure 4C; Supplementary Figure 3B, lower panel). Applying Ub-POD to
347 CHIP demonstrated that a flexible linker between BirA and the candidate Ub ligase can improve
348 the identification of substrates and that biotin exposure times may need to be optimized for a
349 given Ub ligase to identify different sets of substrates.
350 As observed for Rad18 (Figure 2D), PR619 treatment improved the efficiency of substrate
351 identification for CHIP. CHIP-GSGS-BirA-HA transfected cells were treated with 10 μM of PR619,
352 2 hours post MG132 treatment (10 μM) . Proteomics analysis showed that compared to MG132
353 treatment alone (Figure 4C), MG132 and PR619 co-treatment not only increased the overall
354 number of identified targets and the fold change of identified hits (Figure 4D), but also resulted in
355 the identification of more known substrates of CHIP, such as CTNNB1(*15*) and HSPA4(*59*)
356 (Supplementary table 9,10).
357 Next, we compared the putative CHIP substrates identified by Ub-POD to the ones previously
358 identified through an orthogonal ubiquitin transfer (OUT) screen(*15*). Among the 311 potential
359 CHIP substrates identified by Ub-POD, 30 proteins overlapped with the 226 putative CHIP
360 substrates found in the OUT screen (Supplementary Figure 3C; Supplementary table 11). Of
361 these 30 overlapping proteins, only SQSTM1/p62 and CTNNB1 were already known substrates
362 of CHIP. However, two other well-known substrates of CHIP, SOD2 and HIF1, which were
363 identified by Ub-POD, were not found in the OUT screen for CHIP.
364 Moreover, Annexin 5 (ANXA5), a member of the annexin superfamily of proteins, was identified
365 by Ub-POD (in different biotin exposure regimes) as well as by OUT screen. Annexins are a family
366 of cytosolic proteins that translocate to the plasma membrane in a calcium-dependent manner
367 and thus regulates actin cytoskeleton dynamics(*60*). Intriguingly, a previous report found that
368 ANXA5 is upregulated in CHIP KO cortical neurons compared to CHIP expressing neurons(*61*).
369 Based on this, we hypothesize that ANXA5 is a possible substrate of CHIP ligase.
370
371 **Discussion**
372 Here, we developed a new approach to effectively label the substrates of a given ubiquitin
373 ligase with biotin directly in cells and identify them using quantitative mass spectrometry. It is
374 worth mentioning that our approach has important differences from the traditional proximity

375 labeling approaches such as BioID and TurboID, which have been successfully employed in a
376 number of studies to identify interacting partners of a protein of interest (POI)(*25*, *26*). The BioID
377 method involves the expression of the protein of interest tagged with a mutant of BirA, called BirA*
378 or BioID, which bears the mutation R118G in the active site of the enzyme. BirA* releases highly
379 reactive biotin-AMP conjugate into solvent which can label any protein within the spherical radius
380 of ~10nm, thus providing a clear picture of the interactors and the environment of the POI.
381 However, BioID does not differentiated between the direct interactor and any other protein within
382 the vicinity of the POI. In the context of E3 ligases, BioID would also not be able to differentiate
383 between the substrate of the ligase and an interactor of the ligase. We introduced two essential
384 tweaks into the principle of BioID to make it selective for ubiquitin (Ub). Firstly, we fused the
385 wildtype BirA enzyme, which can only efficiently biotinylate the lysine present in the acceptor
386 peptide (AP) or Avi tag, to the E3 ligase of interest. Secondly, we attached a variant of AP tag ((-
387 2)AP) to the N-terminus of Ub to be selectively biotinylated by wildtype BirA in a proximity-
388 dependent manner in the course of substrate ubiquitination (Figure 1A-B). Ub-POD also works
389 based on the location of the catalytic domain in the E3 ligase, since according to the catalytic
390 intermediate complex structures(*19*, *23*, *24*, *62*) (Supplementary Figure 1A, 1B), fusion of BirA to
391 the opposite end of the protein relative to the catalytic domain likely places it too far from the (-
392 2)AP-Ub~E2. For efficient biotinylation, we fused BirA to the N-terminus of Rad18, which
393 possesses a RING domain at the N-terminus, and to the C-terminus of CHIP, which contains U-
394 box domain at the C-terminus. We expect that these tagging principles are widely applicable to
395 other E3 ligases as well. Intriguingly, we also observed that the linker between the BirA and the
396 E3 ligase also plays an important role in determining the efficiency of the Ub-POD. By increasing
397 the linker length in the case of CHIP, we were able to increase the biotinylation (Figure 4).
398 Furthermore, we discovered that both the timing of biotin addition to the cells relative to the
399 expression of the BirA tagged ligase and the duration of biotin exposure can also be important
400 parameters that can be varied, depending on the E3 ligase of interest (as is the case of CHIP,
401 Figure 4, Supplementary figure 3), to allow the detection of different sets of substrates for a given
402 E3 ligase.
403 The primary condition for the success of Ub-POD for a given ubiquitin ligase is that the
404 ligase-mediated substrate ubiquitination should occur and be preserved until isolation in the cell
405 line of choice and under the conditions employed. Use of appropriate triggers, such as UV for
406 Rad18, should be considered for activating ligases. For preserving the ubiquitination and to
407 prevent Ub recycling, the use of MG132 and/or PR619 or other similar agents should be
408 considered. For substrate identification through proteomics, we primarily expressed HA-BirA

409 alone without the candidate ligase fusion as a control. The successful use of HA-BirA as a control
410 for multiple ligases here also implies that it could serve as an efficient control, in principle, for
411 other RING or U-Box E3 ligases. Where known, point mutants of ligases lacking the catalytic
412 activity can also be used as controls. To summarize these general principles of Ub-POD, we
413 prepared a simple flow chart that should guide future Ub-POD experiments targeting various E3
414 ligases (Figure 5).

415 Several available methods can also be employed to identify the substrates of ubiquitin
416 ligases(*6*, *7*). Although the gold standard methods, such as diGly and GPS profiling (specific for
417 degradative ubiquitination), are very effective in the identification of ligase substrates, they are
418 resource intensive and require acquired expertise to employ(*8–10*). Simpler methods similar to
419 Ub-POD that trap the substrate of ubiquitin ligases also exist, such as UBAIT or TULIP, which
420 depend on the fusion of Ub to the ligase to covalently trap the ligase-substrate complex(*11*, *13*).
421 These methods depend on the ability of the ligase to use the Ub-ligase fusion, which is quite bulky
422 compared to Ub alone, in the Ub-cascade reaction. Any laboratory with access to basic tissue
423 culture and a mass spectrometry facility would be able to employ Ub-POD. Moreover, the (-2) AP-
424 tag on Ub is very small compared to the Ub-ligase fusion employed in UBAIT and related
425 approaches. Ub-POD also enables the isolation of potential substrates in harsh denaturing
426 conditions which extracts proteins residing in typically insoluble cellular fractions and also limits
427 the number of false positive hits. Finally, Ub-POD provides a unique opportunity to visualize the
428 cellular localization of ubiquitination by a ligase of interest, offering a peek into the cellular function
429 of the ligase.

430 In the current study, we demonstrated the use of Ub-POD on two classes of E3 ligases, RING
431 and U-box. RING-type E3 ligases comprise the majority of ubiquitin ligases in humans and using
432 the principles described in this discussion and Figure 5, it could be possible to apply Ub-POD for
433 substrate identification of all of ~600 RING E3 ligases. Although not part of this study, we predict
434 that Ub-POD can be employed for HECT or RBR E3 ligases, which also operate on principles of
435 complexing with Ub before the transfer of Ub to the substrate. In the case of HECT or RBR E3
436 ligases, the catalytic cysteine that forms a covalent thioester intermediate with Ub could be
437 mutated to alanine to serve as an ideal control for the proteomics experiment. Ubiquitin-like
438 molecules (UBLs) such as SUMO, NEDD8, FAT10, ISG15 and UFM1 are also conjugated to
439 proteins in a similar fashion to Ub, using a near-identical cascade of enzymatic reactions(*63*). By
440 tagging the respective ligases with BirA and UBL with (-2)AP tag, Ub-POD can in principle be
441 adapted to other UBLs as well. In light of the demonstrated applications and possible other
442 applications discussed here, Ub-POD likely will play an important role in future ubiquitin research.

443

444 **Figure legends**

445 **Figure 1: Employing Ub-POD to identify substrates of RING E3 ligase Rad18**

446 A) Structural model of ubiquitin conjugating enzyme-E2 (yellow), ubiquitin ligase-E3 (RING)
447 (green) and ubiquitin (red) in complex. Placing AP tag at the N terminus of Ub and BirA at the
448 catalytic end of RING-E3 ligase bring them in proximity (21Å) to each other.

449 B) Schematic representation of the Ub-POD method.

450 C) (left panel) Rad18-Ub-POD experimental details with constructs used and inducer treatment
451 regimes; (right panel) HEK-293 cells were transfected with either wt-HA-BirA-Rad18 or HA-BirA-
452 Rad18(C64D), alongwith AP-Ub construct and further exposed to UV (10 miliJoules/cm2) as
453 shown in figure 1C left panel. UV untreated cells were taken as control. Harvested cell lysates
454 were subjected to SDS-PAGE and immunoblotting.

455 D) Volcano plot showing comparison of identified proteins between streptavidin IPed samples (n=
456 3 biological replicates) of wt-HA-BirA-Rad18 expressing HEK-293 cells in absence or presence
457 of UV exposure. Hits [p value < 0.05, log2FC > 0.6] have been colored in red and known Rad18
458 substrates have been marked.

459

460 **Figure 2: A variant of AP-tag increases the efficiency of UbPOD**

461 A) (upper panel) Amino acid substitutions of different AP-tag variants compared to wt AP-tag;
462 (lower panel) Experimental detail of optimization of different AP-tag variants.

463 B) HA-BirA-Rad18 transfected HEK-293 cells were co-transfected with different AP tag variants.
464 Only AP-tag variants overexpressed HEK-293 cells were taken as controls. Both counterparts
465 were treated as shown in 2A, lower panel. Cell lysates prepared after indicated treatments were
466 subjected to SDS-PAGE and western blotting.

467 C) (left panel) (-2)-AP-Ub transfected HEK-293 cells were co transfected with either HA-BirA or
468 HA-BirA-Rad18 (in presence of 100uM biotin). After UV exposure and further biotin treatment,
469 streptavidin IP was done with the harvested cell lysates followed by proteomics analysis (n=3
470 biological replicates). Volcano plot shows the log2 fold change of altered biotinylated proteins in
471 the HA-BirA-Rad18[+UV] / HA-BirA[+UV] counterparts. Proteins with p value < 0.05, log2FC > 0.6
472 were considered as hits (red). Known as well as putative potential substrates of Rad18 has been
473 marked; (right panel) GO-annotation analysis was done with the identified hits. Dot size and dot
474 color shows the number of proteins and FDR values respectively.

475 D) (left panel) HEK-293 cells were transfected as described in 2C, PR619 (10uM) treatment was
476 done after 2 hours of UV exposure to the HA-BirA-Rad18 counterpart. Similarly, HA-BirA

477 transfected cells were treated with vehicle (DMSO). Proteomics analysis was done with the
478 streptividin-IPed samples (n=3 biological replicates) and comparison of the identified proteins in
479 two conditions have been represented as volcano plot [p value < 0.05, log2FC > 0.6 have been
480 considered as cutoffs for hits (red)] ; (right panel) GO annotation analysis has been done with the
481 identified hits as mentioned before (dot size and dot color shows the number of proteins and FDR
482 values respectively).
483 E) HEK-293 cells were treated as shown in the figure followed by fixation. Double immunostaining
484 was done with anti-HA (green) and anti-streptavidin (red) antibodies. DAPI was used to stain
485 nucleus (blue). Scale bar 12μm.
486 F) Quantification of the experiment shown in Figure 2E. Percentage of transfected cells with UV-
487 irradiation induced foci were counted as described in the methods for both HA-BirA and HA-BirA-
488 Rad18 and plotted (****p<0.0001) (n= 6 different fields).
489 G) Pearson correlation coefficient was measured to depict the colocalization between red and
490 green channels for HA-BirA and HA-BirA-Rad18 counterparts and represented as a bar graph (****
491 p<0.0001) (n=20 cells analysed for each condition from different fields).
492
493 **Figure 3: Employing Ub-POD on the RING E3 ligase TRAF6**
494 A) Experimental plan of Ub-POD-TRAF6
495 B) HEK-293 cells transiently overexpressing HA-BirA or HA-BirA-TRAF6 were subjected to Biotin
496 (100 μM) and TNFα treatment (25 ng/ml) for 15 min followed by RIPA lysis and analysis via
497 immunoblotting.
498 C) (left panel) Volcano plot depicting altered biotinylated proteins after enrichment via streptavidin
499 pulldown from HA-BirA-TRAF6 or HA-BirA expressing HEK-293 cells. Known and potential
500 TRAF6 substrates are highlighted. Significantly altered proteins are labeled in dark (FDR<0.05,
501 log2FC > I1I) and light color (FDR<0.05, 0 > I log2FC I < I1I) (two-sided t-test, n = 4 independent
502 experiments); (right panel) GO terms of proteins found to be significantly enriched in HA-BirA-
503 TRAF6 versus HA-BirA with FC ≥1. Dot size correlates to number of proteins, dot color to term
504 enrichment (FDR-value).
505
506 **Figure 4: Employing Ub-POD to identify substrates of U-box ligase CHIP**
507 A) CHIP-Ub-POD experimental plan
508 B) -(2) AP-Ub transfected HEK-293 cells were co-transfected with HA-BirA/ CHIP-BirA-HA/ CHIP-
509 GSGS-BirA-HA/ CHIP (I235DF237D)-BirA-HA in presence of biotin. Next day, cells were treated

510 with MG132 (10uM) and biotin (100uM). After 6 hours, cells were lysed followed by SDS-PAGE
511 and immunoblotting.
512 C) (left panel) HEK-293 cells were transfected with either HA-BirA or CHIP-GSGS-BirA-HA,
513 alongwith -(2) AP-Ub, and treated with MG132 as shown in figure 4A. Streptavidin IP was done
514 with the harvested cell lysates. Comparison of identified biotinylated proteins from streptavidin
515 IPed samples of CHIP-GSGS-BirA-HA/ HA-BirA has been represented as volcano plot (n=3
516 biological replicates; p value < 0.05, log2FC > 0.6 have been colored red and considered as hits);
517 (right panel) GO annotation analysis shows the highlighted biological processes related to
518 identified hits in 4C left panel (dot size= no. of genes; dot color=FDR value).
519 D) HEK-293 cells were transfected with HA-BirA or CHIP-GSGS-BirA-HA as described in figure
520 4C. Next day, after 2 hours of MG132 (10uM) and biotin (100uM) treatment, the CHIP-GSGS-
521 BirA-HA and HA-BirA counterparts were further treated with PR619 (10uM) and vehicle (DMSO),
522 respectively, and incubated for 4 more hours. Streptavidin IP was done with the harvested cell
523 lysates followed by proteomics analysis. log2 fold change of identified proteins in CHIP-GSGS-
524 BirA-HA/HA-BirA has been represented as volcano plot (n=3 biological replicates; p value < 0.05,
525 log2FC > 0.6 have been colored red and considered as hits); (right panel) Identified GO-
526 annotation terms related to identified hits in the proteomics analysis has been represented (dot
527 size= no. of genes; dot colour=FDR value).
528
529 **Supplementary Figure 1:**
530 A) Structural model of RING E3 ligase (green) in complex with ubiquitin conjugating enzyme E2
531 (yellow) and ubiquitin (red). The distance between N terminus of Ub and catalytic RING domain
532 has been shown.
533 B) Structural model of HECT-E3-ligase (green) in complex with Ub (purple) showing the distance
534 between the catalytic HECT domain of HECT-E3 ligase and N terminus of Ub.
535
536 **Supplementary Figure 2:**
537 A) Volcano plot of biotinylated proteins after enrichment via streptavidin pulldown in HA-BirA-
538 TRAF6 expressing HEK-293 cells treated with 25 ng/ml TNFα for 15 min versus mock-treated
539 HA-BirA expressing HEK-293 cells. Known and potential TRAF6 substrates are highlighted.
540 Significantly altered proteins are labeled in dark (FDR<0.05, log2FC > I1I) and light color
541 (FDR<0.05, 0 > I log2FC I < I1I) (two-sided t-test, n = 4 independent experiments).
542 B) Volcano plot depicting differentially enriched biotinylated proteins between TNFα (25 ng/ml, 15
543 min) and mock treated HA-BirA-TRAF6 expressing HEK-293 cells, respectively. Known and

544 potential TRAF6 substrates are labeled in black, proteins with p-value<0.05, log2FC >1 are
545 highlighted. Dark colors highlight protein groups with p-value, log2FC > I1I and light colors with
546 p-value<0.05, 0 > I log2FC I < I1I (two-sided t-test, n = 4 independent experiments).
547
548 **Supplementary figure 3:**
549 A) Experimental plan of shorter biotin treatment regime tested for CHIP-UbPOD.
550 B) (upper panel) HEK-293 cells were treated as described in the plan in supplementary figure 3A.
551 Volcano plot shows the altered biotinylated proteins from CHIP-GSGS-BirA-HA/ HA-BirA
552 counterparts (n=3 biological replicates; p value < 0.05, log2FC > 0.6 are the cutoffs for hits (red));
553 (lower panel) Highlighted GO-annotation terms for the enriched proteins in CHIP-GSGS-BirA-HA
554 counterpart compared to HA-BirA control have been shown (dot size= no. of genes; dot color=
555 FDR value).
556 C) Venn diagram showing overlap of identified proteins in proteomics analysis of CHIP-Ub-POD
557 [Figure 4B (-DUB inhibitor), 4C (+DUB inhibitor) and supplementary figure 3B (shorter biotin
558 exposure)] with CHIP-OUT screen (*15*).
559
560 **Supplementary tables:**
561 **Table S1:** Proteomics for HA-BirA-Rad18 [+UV]/HA-BirA-Rad18 [-UV], Figure 1D.
562 **Table S2:** Proteomics for HA-BirA-Rad18 [+UV] / HA-BirA [+UV] , Figure 2C.
563 **Table S3:** Proteomics for HA-BirA-Rad18 [+UV+PR619] / HA-BirA [+UV] , Figure 2D.
564 **Table S4:** Proteomics for BirA-TRAF6_BirA , Figure 3C.
565 **Table S5:** Proteomics for BirA-TRAF6+TNFa_BirA , Figure S2A.
566 **Table S6:** Proteomics for BirA-TRAF6+TNFa_BirA-TRAF6 , Figure S2B.
567 **Table S7:** Proteomics for CHIP-GSGS-BirA-HA [+MG132]/ HA-BirA [+MG132] , Figure 4C.
568 **Table S8:** Proteomics for CHIP-GSGS-BirA-HA[+MG132]/HA-BirA[+MG132] Shorter (6h) biotin
569 exposure , Figure S3B.
570 **Table S9:** Proteomics for CHIP-GSGS-BirA-HA [+MG132+PR619]/ HA-BirA [+MG132] , Figure
571 4C.
572 **Table S10:** Comparison of Log2fold change of putative CHIP substrates in absence or presence
573 of PR619.
574 **Table S11:** Common CHIP substrates identified by CHIP-Ub-POD and CHIP-OUT (15).
575
576 **References:**

1. R. J. Deshaies, C. A. P. Joazeiro, RING domain E3 ubiquitin ligases. *Annu Rev Biochem*. **78**, 399–434 (2009).

2. W. Li, M. H. Bengtson, A. Ulbrich, A. Matsuda, V. A. Reddy, A. Orth, S. K. Chanda, S. Batalov, C. A. P. Joazeiro, Genome-Wide and Functional Annotation of Human E3 Ubiquitin Ligases Identifies MULAN, a Mitochondrial E3 that Regulates the Organelle's Dynamics and Signaling. *PLOS ONE*. **3**, e1487 (2008).

3. S. Hatakeyama, M. Yada, M. Matsumoto, N. Ishida, K. I. Nakayama, U box proteins as a new family of ubiquitin-protein ligases. *J Biol Chem*. **276**, 33111–33120 (2001).

4. F. E. Morreale, H. Walden, Types of Ubiquitin Ligases. *Cell*. **165**, 248-248.e1 (2016).

5. X. Wang, Y. Li, M. He, X. Kong, P. Jiang, X. Liu, L. Diao, X. Zhang, H. Li, X. Ling, S. Xia, Z. Liu, Y. Liu, C.-P. Cui, Y. Wang, L. Tang, L. Zhang, F. He, D. Li, UbiBrowser 2.0: a comprehensive resource for proteome-wide known and predicted ubiquitin ligase/deubiquitinase-substrate interactions in eukaryotic species. *Nucleic Acids Res*. **50**, D719–D728 (2022).

6. M. Iconomou, D. N. Saunders, Systematic approaches to identify E3 ligase substrates. *Biochem J*. **473**, 4083–4101 (2016).

7. B. Zhao, Y. C. Tsai, B. Jin, B. Wang, Y. Wang, H. Zhou, T. Carpenter, A. M. Weissman, J. Yin, Protein Engineering in the Ubiquitin System: Tools for Discovery and Beyond. *Pharmacol Rev*. **72**, 380–413 (2020).

8. W. Kim, E. J. Bennett, E. L. Huttlin, A. Guo, J. Li, A. Possemato, M. E. Sowa, R. Rad, J. Rush, M. J. Comb, J. W. Harper, S. P. Gygi, Systematic and quantitative assessment of the ubiquitin-modified proteome. *Mol Cell*. **44**, 325–340 (2011).

9. H.-C. S. Yen, S. J. Elledge, Identification of SCF ubiquitin ligase substrates by global protein stability profiling. *Science*. **322**, 923–929 (2008).

10. H.-C. S. Yen, Q. Xu, D. M. Chou, Z. Zhao, S. J. Elledge, Global protein stability profiling in mammalian cells. *Science*. **322**, 918–923 (2008).

11. H. F. O'Connor, N. Lyon, J. W. Leung, P. Agarwal, C. D. Swaim, K. M. Miller, J. M. Huibregtse, Ubiquitin-Activated Interaction Traps (UBAITs) identify E3 ligase binding partners. *EMBO reports*. **16**, 1699–1712 (2015).

12. R. Kumar, R. González-Prieto, Z. Xiao, M. Verlaan-de Vries, A. C. O. Vertegaal, The STUbL RNF4 regulates protein group SUMOylation by targeting the SUMO conjugation machinery. *Nat Commun*. **8**, 1809 (2017).

13. D. Salas-Lloret, G. Agabitini, R. González-Prieto, TULIP2: An Improved Method for the Identification of Ubiquitin E3-Specific Targets. *Frontiers in Chemistry*. **7** (2019) (available at https://www.frontiersin.org/articles/10.3389/fchem.2019.00802).

14. G. Bakos, L. Yu, I. A. Gak, T. I. Roumeliotis, D. Liakopoulos, J. S. Choudhary, J. Mansfeld, An E2-ubiquitin thioester-driven approach to identify substrates modified with ubiquitin and ubiquitin-like molecules. *Nat Commun*. **9**, 4776 (2018).

615 15. K. Bhuripanyo, Y. Wang, X. Liu, L. Zhou, R. Liu, D. Duong, B. Zhao, Y. Bi, H. Zhou, G.
616 Chen, N. T. Seyfried, W. J. Chazin, H. Kiyokawa, J. Yin, Identifying the substrate proteins
617 of U-box E3s E4B and CHIP by orthogonal ubiquitin transfer. *Sci Adv*. **4**, e1701393 (2018).

618 16. Y. Wang, X. Liu, L. Zhou, D. Duong, K. Bhuripanyo, B. Zhao, H. Zhou, R. Liu, Y. Bi, H.
619 Kiyokawa, J. Yin, Identifying the ubiquitination targets of E6AP by orthogonal ubiquitin
620 transfer. *Nat Commun*. **8**, 2232 (2017).

621 17. R. Gupta, B. Kus, C. Fladd, J. Wasmuth, R. Tonikian, S. Sidhu, N. J. Krogan, J. Parkinson,
622 D. Rotin, Ubiquitination screen using protein microarrays for comprehensive identification
623 of Rsp5 substrates in yeast. *Mol Syst Biol*. **3**, 116 (2007).

624 18. M. Zhuang, S. Guan, H. Wang, A. L. Burlingame, J. A. Wells, Substrates of IAP ubiquitin
625 ligases identified with a designed orthogonal E3 ligase, the NEDDylator. *Mol Cell*. **49**, 273–
626 282 (2013).

627 19. A. Plechanovová, E. G. Jaffray, M. H. Tatham, J. H. Naismith, R. T. Hay, Structure of a
628 RING E3 ligase and ubiquitin-loaded E2 primed for catalysis. *Nature*. **489**, 115–120 (2012).

629 20. E. Branigan, A. Plechanovová, E. G. Jaffray, J. H. Naismith, R. T. Hay, Structural basis for
630 the RING-catalyzed synthesis of K63-linked ubiquitin chains. *Nat Struct Mol Biol*. **22**, 597–
631 602 (2015).

632 21. K. L. Lorick, J. P. Jensen, S. Fang, A. M. Ong, S. Hatakeyama, A. M. Weissman, RING
633 fingers mediate ubiquitin-conjugating enzyme (E2)-dependent ubiquitination. *Proc Natl*
634 *Acad Sci U S A*. **96**, 11364–11369 (1999).

635 22. P. D. Mace, K. Linke, R. Feltham, F.-R. Schumacher, C. A. Smith, D. L. Vaux, J. Silke, C. L.
636 Day, Structures of the cIAP2 RING domain reveal conformational changes associated with
637 ubiquitin-conjugating enzyme (E2) recruitment. *J Biol Chem*. **283**, 31633–31640 (2008).

638 23. H. B. Kamadurai, Y. Qiu, A. Deng, J. S. Harrison, C. MacDonald, M. Actis, P. Rodrigues, D.
639 J. Miller, J. Souphron, S. M. Lewis, I. Kurinov, N. Fujii, M. Hammel, R. Piper, B. Kuhlman,
640 B. A. Schulman, Mechanism of ubiquitin ligation and lysine prioritization by a HECT E3.
641 *eLife*. **2**, e00828 (2013).

642 24. E. Maspero, E. Valentini, S. Mari, V. Cecatiello, P. Soffientini, S. Pasqualato, S. Polo,
643 Structure of a ubiquitin-loaded HECT ligase reveals the molecular basis for catalytic
644 priming. *Nat Struct Mol Biol*. **20**, 696–701 (2013).

645 25. K. F. Cho, T. C. Branon, N. D. Udeshi, S. A. Myers, S. A. Carr, A. Y. Ting, Proximity labeling
646 in mammalian cells with TurboID and split-TurboID. *Nat Protoc*. **15**, 3971–3999 (2020).

647 26. K. J. Roux, D. I. Kim, M. Raida, B. Burke, A promiscuous biotin ligase fusion protein
648 identifies proximal and interacting proteins in mammalian cells. *J Cell Biol*. **196**, 801–810
649 (2012).

650 27. K. Kido, S. Yamanaka, S. Nakano, K. Motani, S. Shinohara, A. Nozawa, H. Kosako, S. Ito,
651 T. Sawasaki, AirID, a novel proximity biotinylation enzyme, for analysis of protein–protein
652 interactions. *eLife*. **9**, e54983 (2020).

653 28. D. Beckett, E. Kovaleva, P. J. Schatz, A minimal peptide substrate in biotin holoenzyme
654 synthetase-catalyzed biotinylation. *Protein Sci*. **8**, 921–929 (1999).

655 29. C. Hoege, B. Pfander, G.-L. Moldovan, G. Pyrowolakis, S. Jentsch, RAD6-dependent DNA
656 repair is linked to modification of PCNA by ubiquitin and SUMO. *Nature*. **419**, 135–141
657 (2002).

658 30. Y. Gao, E. Mutter-Rottmayer, A. M. Greenwalt, D. Goldfarb, F. Yan, Y. Yang, R. C.
659 Martinez-Chacin, K. H. Pearce, S. Tateishi, M. B. Major, C. Vaziri, A neomorphic cancer
660 cell-specific role of MAGE-A4 in trans-lesion synthesis. *Nat Commun*. **7**, 12105 (2016).

661 31. M. Fernández-Suárez, T. S. Chen, A. Y. Ting, Protein−Protein Interaction Detection in Vitro
662 and in Cells by Proximity Biotinylation. *J. Am. Chem. Soc.* **130**, 9251–9253 (2008).

663 32. Y. Li, P. Xie, L. Lu, J. Wang, L. Diao, Z. Liu, F. Guo, Y. He, Y. Liu, Q. Huang, H. Liang, D. Li,
664 F. He, An integrated bioinformatics platform for investigating the human E3 ubiquitin
665 ligase-substrate interaction network. *Nat Commun*. **8**, 347 (2017).

666 33. Y. Baris, M. R. G. Taylor, V. Aria, J. T. P. Yeeles, Fast and efficient DNA replication with
667 purified human proteins. *Nature*. **606**, 204–210 (2022).

668 34. L. K. Povlsen, P. Beli, S. A. Wagner, S. L. Poulsen, K. B. Sylvestersen, J. W. Poulsen, M. L.
669 Nielsen, S. Bekker-Jensen, N. Mailand, C. Choudhary, Systems-wide analysis of
670 ubiquitylation dynamics reveals a key role for PAF15 ubiquitylation in DNA-damage
671 bypass. *Nat Cell Biol*. **14**, 1089–1098 (2012).

672 35. S. M. B. Nijman, M. P. A. Luna-Vargas, A. Velds, T. R. Brummelkamp, A. M. G. Dirac, T. K.
673 Sixma, R. Bernards, A genomic and functional inventory of deubiquitinating enzymes. *Cell*.
674 **123**, 773–786 (2005).

675 36. M. Hu, P. Li, L. Song, P. D. Jeffrey, T. A. Chenova, K. D. Wilkinson, R. E. Cohen, Y. Shi,
676 Structure and mechanisms of the proteasome-associated deubiquitinating enzyme USP14.
677 *EMBO J*. **24**, 3747–3756 (2005).

678 37. M. Altun, H. B. Kramer, L. I. Willems, J. L. McDermott, C. A. Leach, S. J. Goldenberg, K. G.
679 S. Kumar, R. Konietzny, R. Fischer, E. Kogan, M. M. Mackeen, J. McGouran, S. V.
680 Khoronenkova, J. L. Parsons, G. L. Dianov, B. Nicholson, B. M. Kessler, Activity-based
681 chemical proteomics accelerates inhibitor development for deubiquitylating enzymes.
682 *Chem Biol*. **18**, 1401–1412 (2011).

683 38. R. Oughtred, J. Rust, C. Chang, B. Breitkreutz, C. Stark, A. Willems, L. Boucher, G. Leung,
684 N. Kolas, F. Zhang, S. Dolma, J. Coulombe-Huntington, A. Chatr-aryamontri, K. Dolinski,
685 M. Tyers, The BioGRID database: A comprehensive biomedical resource of curated
686 protein, genetic, and chemical interactions. *Protein Sci*. **30**, 187–200 (2021).

687 39. A. Fabregat, K. Sidiropoulos, G. Viteri, O. Forner, P. Marin-Garcia, V. Arnau, P.
688 D'Eustachio, L. Stein, H. Hermjakob, Reactome pathway analysis: a high-performance in-
689 memory approach. *BMC Bioinformatics*. **18**, 142 (2017).

690 40. K. Watanabe, S. Tateishi, M. Kawasuji, T. Tsurimoto, H. Inoue, M. Yamaizumi, Rad18
691 guides poleta to replication stalling sites through physical interaction and PCNA
692 monoubiquitination. *EMBO J*. **23**, 3886–3896 (2004).

693 41. T. Dainichi, R. Matsumoto, A. Mostafa, K. Kabashima, Immune Control by TRAF6-Mediated
694 Pathways of Epithelial Cells in the EIME (Epithelial Immune Microenvironment). *Front*
695 *Immunol*. **10**, 1107 (2019).

696 42. L. Deng, C. Wang, E. Spencer, L. Yang, A. Braun, J. You, C. Slaughter, C. Pickart, Z. J.
697 Chen, Activation of the IkappaB kinase complex by TRAF6 requires a dimeric ubiquitin-
698 conjugating enzyme complex and a unique polyubiquitin chain. *Cell*. **103**, 351–361 (2000).

699 43. B. Lamothe, A. Besse, A. D. Campos, W. K. Webster, H. Wu, B. G. Darnay, Site-specific
700 Lys-63-linked tumor necrosis factor receptor-associated factor 6 auto-ubiquitination is a
701 critical determinant of I kappa B kinase activation. *J Biol Chem*. **282**, 4102–4112 (2007).

702 44. Z.-P. Xia, L. Sun, X. Chen, G. Pineda, X. Jiang, A. Adhikari, W. Zeng, Z. J. Chen, Direct
703 activation of protein kinases by unanchored polyubiquitin chains. *Nature*. **461**, 114–119
704 (2009).

705 45. D. B. Conze, C.-J. Wu, J. A. Thomas, A. Landstrom, J. D. Ashwell, Lys63-Linked
706 Polyubiquitination of IRAK-1 Is Required for Interleukin-1 Receptor- and Toll-Like
707 Receptor-Mediated NF-κB Activation. *Mol Cell Biol*. **28**, 3538–3547 (2008).

708 46. K. Yan, L. Li, X. Wang, R. Hong, Y. Zhang, H. Yang, M. Lin, S. Zhang, Q. He, D. Zheng, J.
709 Tang, Y. Yin, G. Shao, The deubiquitinating enzyme complex BRISC is required for proper
710 mitotic spindle assembly in mammalian cells. *J Cell Biol*. **210**, 209–224 (2015).

711 47. H. Chanut-Delalande, A. C. Jung, M. M. Baer, L. Lin, F. Payre, M. Affolter, The Hrs/Stam
712 Complex Acts as a Positive and Negative Regulator of RTK Signaling during Drosophila
713 Development. *PLOS ONE*. **5**, e10245 (2010).

714 48. L. Aravind, E. V. Koonin, The U box is a modified RING finger - a common domain in
715 ubiquitination. *Curr Biol*. **10**, R132-134 (2000).

716 49. M. D. Ohi, C. W. Vander Kooi, J. A. Rosenberg, W. J. Chazin, K. L. Gould, Structural
717 insights into the U-box, a domain associated with multi-ubiquitination. *Nat Struct Biol*. **10**,
718 250–255 (2003).

719 50. C. A. Ballinger, P. Connell, Y. Wu, Z. Hu, L. J. Thompson, L. Y. Yin, C. Patterson,
720 Identification of CHIP, a novel tetratricopeptide repeat-containing protein that interacts with
721 heat shock proteins and negatively regulates chaperone functions. *Mol Cell Biol*. **19**, 4535–
722 4545 (1999).

723 51. P. Connell, C. A. Ballinger, J. Jiang, Y. Wu, L. J. Thompson, J. Höhfeld, C. Patterson, The
724 co-chaperone CHIP regulates protein triage decisions mediated by heat-shock proteins.
725 *Nat Cell Biol*. **3**, 93–96 (2001).

726 52. S. Murata, Y. Minami, M. Minami, T. Chiba, K. Tanaka, CHIP is a chaperone-dependent E3
727 ligase that ubiquitylates unfolded protein. *EMBO Rep*. **2**, 1133–1138 (2001).

728 53. M. Zhang, M. Windheim, S. M. Roe, M. Peggie, P. Cohen, C. Prodromou, L. H. Pearl,
729 Chaperoned Ubiquitylation—Crystal Structures of the CHIP U Box E3 Ubiquitin Ligase and
730 a CHIP-Ubc13-Uev1a Complex. *Molecular Cell*. **20**, 525–538 (2005).

731 54. J. V. Ferreira, H. Fôfo, E. Bejarano, C. F. Bento, J. S. Ramalho, H. Girão, P. Pereira,
732 STUB1/CHIP is required for HIF1A degradation by chaperone-mediated autophagy.
733 *Autophagy*. **9**, 1349–1366 (2013).

734 55. W. H. Choi, Y. Yun, S. Park, J. H. Jeon, J. Lee, J. H. Lee, S.-A. Yang, N.-K. Kim, C. H.
735 Jung, Y. T. Kwon, D. Han, S. M. Lim, M. J. Lee, Aggresomal sequestration and STUB1-
736 mediated ubiquitylation during mammalian proteaphagy of inhibited proteasomes. *Proc*
737 *Natl Acad Sci U S A*. **117**, 19190–19200 (2020).

738 56. T. Wang, W. Wang, Q. Wang, R. Xie, A. Landay, D. Chen, The E3 ubiquitin ligase CHIP in
739 normal cell function and in disease conditions. *Ann N Y Acad Sci*. **1460**, 3–10 (2020).

740 57. W. Wang, Y. Yang, Y. Shi, T. Xiang, J. Xie, E3 ubiquitin ligase STUB1 affects the mTORC1
741 pathway through p62 and participates in regulating the differentiation of follicular helper T
742 cells in rheumatoid arthritis. *Clin Immunol*. **255**, 109736 (2023).

743 58. S. Zemanovic, M. V. Ivanov, L. V. Ivanova, A. Bhatnagar, T. Michalkiewicz, R.-J. Teng, S.
744 Kumar, R. Rathore, K. A. Pritchard, G. G. Konduri, A. J. Afolayan, Dynamic
745 Phosphorylation of the C Terminus of Hsp70 Regulates the Mitochondrial Import of SOD2
746 and Redox Balance. *Cell Rep*. **25**, 2605-2616.e7 (2018).

747 59. S.-B. Qian, L. Waldron, N. Choudhary, R. E. Klevit, W. J. Chazin, C. Patterson, Engineering
748 a ubiquitin ligase reveals conformational flexibility required for ubiquitin transfer. *J Biol*
749 *Chem*. **284**, 26797–26802 (2009).

750 60. E. Tzima, P. J. Trotter, M. A. Orchard, J. H. Walker, Annexin V relocates to the platelet
751 cytoskeleton upon activation and binds to a specific isoform of actin. *Eur J Biochem*. **267**,
752 4720–4730 (2000).

753 61. C. Dias, E. Nita, J. Faktor, A. C. Tynan, L. Hernychova, B. Vojtesek, J. Nylandsted, T. R.
754 Hupp, T. Kunath, K. L. Ball, CHIP-dependent regulation of the actin cytoskeleton is linked
755 to neuronal cell membrane integrity. *iScience*. **24**, 102878 (2021).

756 62. B. C. Lechtenberg, A. Rajput, R. Sanishvili, M. K. Dobaczewska, C. F. Ware, P. D. Mace, S.
757 J. Riedl, Structure of a HOIP/E2~ubiquitin complex reveals RBR E3 ligase mechanism and
758 regulation. *Nature*. **529**, 546–550 (2016).

759 63. L. Cappadocia, C. D. Lima, Ubiquitin-like Protein Conjugation: Structures, Chemistry, and
760 Mechanism. *Chem. Rev.* **118**, 889–918 (2018).

761 64. C. S. Hughes, S. Foehr, D. A. Garfield, E. E. Furlong, L. M. Steinmetz, J. Krijgsveld,
762 Ultrasensitive proteome analysis using paramagnetic bead technology. *Mol Syst Biol*. **10**,
763 757 (2014).

764 65. C. S. Hughes, S. Moggridge, T. Müller, P. H. Sorensen, G. B. Morin, J. Krijgsveld, Single-
765 pot, solid-phase-enhanced sample preparation for proteomics experiments. *Nat Protoc*. **14**,
766 68–85 (2019).

66. T. Werner, G. Sweetman, M. F. Savitski, T. Mathieson, M. Bantscheff, M. M. Savitski, Ion coalescence of neutron encoded TMT 10-plex reporter ions. *Anal Chem*. **86**, 3594–3601 (2014).

67. M. Reichel, Y. Liao, M. Rettel, C. Ragan, M. Evers, A.-M. Alleaume, R. Horos, M. W. Hentze, T. Preiss, A. A. Millar, In Planta Determination of the mRNA-Binding Proteome of Arabidopsis Etiolated Seedlings. *Plant Cell*. **28**, 2435–2452 (2016).

68. H. Franken, T. Mathieson, D. Childs, G. M. A. Sweetman, T. Werner, I. Tögel, C. Doce, S. Gade, M. Bantscheff, G. Drewes, F. B. M. Reinhard, W. Huber, M. M. Savitski, Thermal proteome profiling for unbiased identification of direct and indirect drug targets using multiplexed quantitative mass spectrometry. *Nat Protoc*. **10**, 1567–1593 (2015).

69. S. X. Ge, D. Jung, R. Yao, ShinyGO: a graphical gene-set enrichment tool for animals and plants. *Bioinformatics*. **36**, 2628–2629 (2020).

Acknowledgements:

We thank the EMBL Mass spectrometry core facility, especially Mandy Rettel for the data acquisition and analysis, Martin Pelosse for training and maintenance of the EMBL eukaryotic expression facility, This work used the platforms of the Grenoble Instruct-ERIC center (ISBG; UAR 3518 CNRS-CEA-UGA-EMBL) within the Grenoble Partnership for Structural Biology (PSB), supported by FRISBI (ANR-10-INBS-0005-02) and GRAL, financed within the University Grenoble Alpes graduate school (Écoles Universitaires de Recherche) CBH-EUR-GS (ANR-17-EURE-0003). SB was supported by a grant from the French Agence Nationale de la Recherche (ANR-21-CE11-0013). UM was supported by EMBO Postdoctoral Fellowship (EMBO-ALTF-185-2021). CB was supported by the Deutsche Forschungsgemeinschaft (DFG, German Research Foundation) within the frameworks of the Munich Cluster for Systems Neurology (EXC 2145 SyNergy – ID 390857198 (C.B.) and the Collaborative Research Center (CRC) 1177 (ID 259130777).

Author Contributions: UM performed Ub-POD experiments with Rad18 and CHIP. SL performed Ub-POD experiments with TRAF6. SG assisted in initial Ub-POD experiments. FS analyzed the mass spectrometry data. CB conceptualized Ub-POD on TRAF6 and supervised SL. SB conceptualized the study and supervised UM. SL, CB, UM, and SB wrote the manuscript.

800 **Competing interests:**

801 The authors declare no competing interests.

802

803 **Materials and methods:**

804 **Cell culture**

805 Human embryonic kidney epithelial cell line 293 [HEK-293] (ATCC CRL-1573) was cultured in
806 Dulbecco's Modified Eagle Medium (DMEM), supplemented with 10% (*v*/*v*) heat-inactivated Fetal
807 Bovine Serum (FBS; Gibco™) within humidified 5% CO_2 incubator at 37°C. The cell line used in
808 this study was free from mycoplasma contamination based on PCR detection.

809

810 **Reagents and antibodies**

811 All reagents used in this study are listed in Table 1 and reconstituted according to manufacturers'
812 instructions. Polyclonal and monoclonal antibodies used for this study are listed in Table 2 and
813 were used according to the manufacturers' recommended dilutions.

Reagent	Manufacturer	Catalog	Concentration and time of treatment
MG132	Calbiochem	474787	10uM for 6 hour
PR619	Tocris (Biotechne)	4482	10uM for 4 hour
Biotin	Sigma	B4639	100uM for 6hour; 100uM for~30hr

814 Table 1: List of reagents

Antibody	Catalog no.	Manufacturer
Streptavidin	926-32230 926-68079	Licor
HA	3724-S	Cell signaling
Tubulin	NB100-690SS	Bio-Techne Ltd.
Rad18	NB100-61063	Bio-Techne Ltd.
PCNA	sc-56	SantaCruz
Biotin	31852	Pierce
Phospho NF-kB	3031	Cell signalling
Calnexin	ab22595	abcam

815 Table 2: List of antibodies

816 **Cloning**

817 In order to tag the catalytic end of the candidate ligases, two vectors containing wild type E.coli
818 biotin ligase enzyme BirA tagged with HA [HA-BirA for tagging candidate ligases with N terminal
819 catalytic domain and BirA-HA for tagging candidate ligases with C terminal catalytic domain] were
820 made, in which the candidate E3 ligases can be cloned based on the position of the catalytic
821 domain. Full-length RAD18, CHIP and TRAF6 was incorporated into required BirA vector by
822 sequence and ligation independent cloning. A GSGS linker was placed in between the catalytic
823 end of candidate ligases and BirA by site directed mutagenesis (SDM). Mutant ligase constructs
824 (either catalytic cysteine mutants or E2-E3 interaction interface mutants) were made also by SDM.
825 Full length Ubiquitin was tagged at its N terminus with an avi tag (AP-Ub). To make truncated AP-
826 Ub constructs (-2)AP-Ub and AP(-3)-Ub, 2 and 3 amino acids from N terminus and C terminus of
827 the Avi tag were truncated, respectively. The list of constructs used in this study are presented in
828 the table 3

HA-BirA
BirA-HA
HA-BirA-Rad18
HA-BirA-Rad18-C64D
CHIP-BirA-HA
CHIP-GSGS-BirA-HA
CHIP(I235DF237A)-BirA-HA
HA-BirA-TRAF6
AP-Ub
(-2)AP-Ub
AP(-3)-Ub

829 Table 3:List of constructs
830
831 **Transient transfection**
832 All plasmids were transfected in HEK-293 cells with Polyethyleneimine (PEI) (Invitrogen)
833 according to the manufacturer's instructions. Briefly, the cells were seeded the day before
834 transfection. Next day, equal amount of Avi-tagged Ub and BirA-tagged candidate ligase
835 constructs were mixed with PEI in a reduced serum medium, the transfection mix was incubated
836 at room temperature for at least 20 minutes before adding dropwise to the cells. The transfected
837 cells were incubated overnight at 37°C, 5% CO_2.
838
839 **Biotin labeling and induction of target protein ubiquitination**

840 Different strategies were taken to induce target protein ubiquitination by the candidate ligases.
841 For Rad18, UV exposure was used as an inducer of DNA damage. For CHIP, the proteasome
842 inhibitor, MG132 was used as an inducer. For TRAF6, TNF α treatment was done.
843 We took two different biotin labelling regimes: a) For shorter biotin exposure, biotin treatment
844 (Supplementary figure 3A, 3B) was done during the inducer (MG132) treatment, 24 hours after
845 transfection. Briefly, the transfection media was removed and replaced with medium
846 supplemented with 100 uM biotin (dissolved in DMEM) and 10uM MG132 and incubated at 37°C,
847 5% CO_2 incubator for 6 hours. b) For all other experiments, biotin treatment was done once during
848 transfection, as well as again during inducer (MG132/TNF α) treatment. Briefly, 24 hours after
849 seeding the cells, the media was removed and replaced with media supplemented with 100 uM
850 biotin followed by transfection. After 24 hours of transfection, the media was removed and
851 replaced with biotin (100uM) as well as MG132 (10uM) /TNF α (25ng/ml) supplemented complete
852 media and incubated at 37°C, 5% CO_2 incubator for times as indicated in figures.
853
854 **UV exposure**
855 For Rad18, UV exposure was used as an inducer. After 24 hours of transfection, the cells were
856 washed in 1X PBS and exposed to UV (10 miliJoules/cm2) in a Stratalinker UV crosslinker oven
857 (Stratagene).After UV exposure, PBS was replaced with biotin (100uM) supplemented complete
858 media and the cells were further incubated for 6 hours of at 37°C, 5% CO_2 incubator.
859
860 **PR619 treatment**
861 For treatment of PR619, the cells were first treated with the inducer, in presence of biotin. After 2
862 hours, 10uM PR619 was added to the media. Equal volume of DMSO was added in mock-treated
863 cells. After 4 hours the cells were harvested.
864
865 **Immunoblotting**
866 After required treatments, the harvested cells were lysed in 1X cell lysis buffer [50 mM Tris-HCl,
867 pH 7.5, 150 mM NaCl, 1% Triton X-100, 0.1%SDS, 250u/ul benzonase, 1mM EGTA, 50mM NEM,
868 protease inhibitor cocktail (Sigma Aldrich)] for 30 minutes at 4 °C. After pelleting the debris, the
869 protein concentrations in the supernatant were measured using a BCA assay (ThermoFisher
870 Scientific). The cell lysates were run on 4-20% Tris glycine gradient gels (Biorad) by SDS-PAGE
871 followed by transfer to polyvinylidenedifluoride (PVDF) membranes. After the transfer, the
872 membranes were incubated in blocking buffer (5% BSA in 1X PBS) for 30 min at room temperature
873 followed by overnight incubation with the antibodies listed in table 2 at 4 °C. Next day, the

874 membranes were incubated with fluorescent tagged secondary antibodies for 45 minutes at RT
875 followed by imaging on a fluorescence scanner imaging system (Biorad).
876
877 **Streptavidin immunoprecipitation and immunoblotting**
878 After required treatments, the harvested cells were lysed in 1X cell lysis buffer [50 mM Tris-HCl,
879 pH 7.5, 150 mM NaCl, 1% Triton X-100, 0.1%SDS, 250u/ul benzonase, 1mM EGTA, 50mM NEM,
880 protease inhibitor cocktail (Sigma Aldrich)] for 30 minutes at 4 °C. After pelleting the debris, the
881 protein concentrations in the supernatant were measured using a BCA assay (ThermoFisher
882 Scientific). For Streptavidin immunoprecipitation, the Streptavidin agarose beads (Thermo) were
883 washed twice with the 1X cell lysis buffer and incubated with 1mg of lysed cell extracts for 2 h at
884 4°C subjected to end-to-end rotation. The beads were washed twice in wash buffer 1 (50 mM
885 Tris-HCl, pH 7.5, 500 mM NaCl, 1%SDS, 1% Triton X-100, 10mM DTT, 1 mM EGTA, 50 mM NEM)
886 and twice more with wash buffer 2 (50 mM Tris-HCl, pH 7.5, 150 mM NaCl, 0.1%SDS, 1% Triton
887 X-100, 10mM DTT, 1 mM EGTA, 50 mM NEM). The final wash was done in wash buffer 3 (50 mM
888 Tris-HCl, pH 7.5, 150 mM NaCl, 50mM NEM). All the washing steps were done for 5 min on a
889 rotation wheel. Proteins were eluted by boiling with 2X gel loading dye. 10% of the elute was kept
890 for immunoblotting and rest was kept for proteomics analysis. Input lysates were also boiled with
891 2X gel loading dye. 20ug of input cell lysates and 10ul of immunoprecipitated elutes were run on
892 4-20% Tris glycine gradient gels (Biorad). For detecting protein biotinylation, the proteins were
893 transferred on a low fluorescence PVDF membrane followed by incubation with fluorescent
894 tagged Streptavidin antibody (1:20,000 dilution in 1X PBS containing 5% BSA, 0.1% Tween-20,
895 0.1%SDS) for 45 min at RT. The membranes were washed three times, each for 5 min, with 1X
896 PBS containing 0.2% Tween-20, and then once more with 1X PBS. The membranes were scanned
897 on a fluorescence scanner imaging system (Biorad).
898
899 **Immunostaining, confocal microscopy and statistical analysis**
900 HEK-293 cells were seeded on 11 mm coverslips coated with poly D lysine in a 6 well plate. The
901 cells were co-transfected with HA-BirA/HA-BirA-Rad18 and (-2)AP-Ub constructs in presence of
902 biotin (100uM). After 16 hours, the cells were exposed to 10 mJ/cm^2 of UV and further incubated
903 for 6 hours in biotin (100uM) containing complete media. The cells were then washed 5 times with
904 1X PBS and fixed with 4% PFA for 20 minutes at RT. After washing 3 times with 1X PBS, cells
905 were blocked and permeabilized in solution 1 (5% BSA, 0.3% Triton X 100 in 1X PBS) for 3 hours
906 at RT. After washing once with 1X PBS, the cells were incubated overnight with anti HA tag
907 primary antibody (1:800) in solution 2 (3% BSA, 0.1% Triton X 100 and 1X PBS). Next day cells

908 were washed 3 times with solution 2 and 2 times with 1X PBS and further incubated with
909 Streptavidin conjugated to Irdye 680 (1:200) and Alexa488 conjugated anti- rabbit Secondary
910 antibody (1:200) for 1 hour in the dark in a humidified 37°C incubator. The cells were then washed
911 5 times with solution 2 and once with 1X PBS before mounting with ProLong antifade mountant
912 with DAPI. Imaging was done in a Leica TCS SP5 confocal microscope (63X oil-immersion
913 objective) keeping all the parameters same throughout the imaging process.
914 For statistical analysis, total no. of transfected cells and the no. of transfected cells with UV-
915 irradiation induced Rad18 foci were counted from 6 different fields for each condition. Percentage
916 difference of transfected cells with UV-irradiation induced Rad18 foci between HA-BirA- Rad18
917 and HA-BirA counterparts were calculated using Graphpad prism 9. Statistical significance of data
918 was calculated by an unpaired T test and is marked as **** for $p<0.0001$. To determine
919 colocalization between Streptavidin (red) and HA-tag (green) images were analysed in FIJI (coloc
920 tool). Results are indicative of 20 cells counted from 10 different images; error bars indicate
921 standard deviation ($p<0.0001$, calculated by unpaired T test).
922
923 **Mass spectrometry and data analysis**
924 Reduction of disulphide bridges in cysteine containing proteins was performed with dithiothreitol
925 (56°C, 30 min, 10 mM in 50 mM HEPES, pH 8.5). Reduced cysteines were alkylated with 2-
926 chloroacetamide (room temperature, in the dark, 30 min, 20 mM in 50 mM HEPES, pH 8.5).
927 Samples were prepared using the SP3 protocol(*63*, *64*) and trypsin (sequencing grade, Promega)
928 was added in an enzyme to protein ratio 1:50 for overnight digestion at 37°C. Next day, peptide
929 recovery was done in HEPES buffer by collecting supernatant on magnet and combining with
930 second elution wash of beads with HEPES buffer. Peptides were labelled with TMT10plex(*65*)
931 Isobaric Label Reagent (Thermo Fisher) according to the manufacturer's instructions. Samples
932 were combined for the TMT10plex and for further sample clean up an OASIS® HLB µElution
933 Plate (Waters) was used.
934 Offline high pH reverse phase fractionation was carried out on an Agilent 1200 Infinity high-
935 performance liquid chromatography system, equipped with a Gemini C18 column (3 µm, 110 Å,
936 100 x 1.0 mm, Phenomenex)(*66*).
937 An UltiMate 3000 RSLC nano LC system (Dionex) fitted with a trapping cartridge (µ-Precolumn
938 C18 PepMap 100, 5µm, 300 µm i.d. x 5 mm, 100 Å) and an analytical column (nanoEase™ M/Z
939 HSS T3 column 75 µm x 250 mm C18, 1.8 µm, 100 Å, Waters) was used. Trapping was carried
940 out with a constant flow of trapping solution (0.05% trifluoroacetic acid in water) at 30 µL/min onto
941 the trapping column for 6 minutes. Subsequently, peptides were eluted via the analytical column

942 running solvent A (0.1% formic acid in water, 3% DMSO) with a constant flow of 0.3 µL/min, with
943 increasing percentage of solvent B (0.1% formic acid in acetonitrile, 3% DMSO) from 2% to 8%
944 in 6 min, then 8% to 28% for a further 66 min, in another 4 min. from 28% to 38%, followed by an
945 increase of B from 38-80% for 3min. and a re-equilibration back to 2% B for 5min. The outlet of
946 the analytical column was coupled directly to an Orbitrap Fusion™ Lumos™ Tribrid™ Mass
947 Spectrometer (Thermo) using the Nanospray Flex™ ion source in positive ion mode. The peptides
948 were introduced into the Orbitrap Fusion Lumos via a Pico-Tip Emitter 360 µm OD x 20 µm ID;
949 10 µm tip (New Objective or CoAnn Technologies) and an applied spray voltage of 2.4 kV. The
950 capillary temperature was set at 275°C. Full mass scan was acquired with mass range 375-1500
951 m/z in profile mode in the orbitrap with resolution of 120000. The filling time was set at maximum
952 of 50 ms with a limitation of 4x105 ions. Data dependent acquisition (DDA) was performed with
953 the resolution of the Orbitrap set to 30000, with a fill time of 94 ms and a limitation of 1x105 ions.
954 A normalized collision energy of 38 was applied. MS2 data was acquired in profile mode.
955 IsobarQuant(*67*) , Mascot (v2.2.07) and MS Fragger were used to process the acquired data. For
956 MS Fragger, all raw files were converted to mzmL format using MSConvert from Proteowizard59,
957 using peak picking from the vendor algorithm. For IsobarQuant and Mascot, the acquired data
958 was searched against Uniprot Homo sapiens proteome (UP000005640) containing common
959 contaminants and reversed sequences. For MS Fragger, files were searched using MSFragger
960 v3.7 (PMID: 28394336) in Fragpipe v19.1 against the Swissprot Homo sapiens (UP000005640)
961 database (20,594 entries) containing common contaminants and reversed sequences. The
962 following modifications were included into the search parameters: Carbamidomethyl (C) and
963 TMT10 (K) (fixed modification), Acetyl (Protein N-term), Oxidation (M) and TMT10 (N-term)
964 (variable modifications). For the full scan (MS1) a mass error tolerance of 10 ppm and for MS/MS
965 (MS2) spectra of 0.02 Da was set. Further parameters were set: Trypsin as protease with an
966 allowance of maximum two missed cleavages: a minimum peptide length of seven amino acids;
967 at least two unique peptides were required for a protein identification. The false discovery rate on
968 peptide and protein level was set to 0.01. GO annotation analysis of the identified hits were
969 performed in ShinyGO(*68*) .
970
971 **Statistical analysis**
972 All experiments were independently reproduced at least two times with similar results obtained.
973 No data were excluded from analysis. Statistical analysis for confocal images was performed by
974 blinding the investigators to group allocation. Data are presented as the mean ± s.d. for bar
975 graphs. P values were calculated using unpaired Student's t-test using graphpad prism v.9.

976

977 **Methods for the TRAF6 Ub-POD**

978 **Biotin, PR-619 and TNFα treatment and harvest for TRAF6 E3 ligase**

979 To induce biotinylation, transfection media was removed and replaced by DMEM supplemented
980 with 100 µM Biotin, 10 µM PR-619 and 25 ng/ml TNFα. Cells were treated at 37 °C, 5% CO_2 for
981 15 min. Mock controls were treated with respective amount of dissolving agent (DMSO).

982

983 **Immunoblotting**

984 For total lysates, cells were lysed in RIPA-buffer (50mM Tris, 150mM NaCl, 0.1% SDS, 0.5%
985 sodium deoxycholate, 1% Triton-X, 50 µM PR-619, 1× protease inhibitors (Roche) and 1×
986 PhosStop (Roche)) for 30 min on ice. After clearance by centrifugation at 20,000 × g for 10 min
987 at 4 °C, protein concentrations were adjusted using BCA assay. Afterwards, lysates were boiled
988 in sample buffer (200mM Tris-HCL, 6% SDS, 20% Glycerol, 0.1 g/ml DTT and 0.01mg
989 Bromophenol Blue) for 5 min at 95 °C. Proteins were separated by SDS-PAGE and transferred
990 onto nitrocellulose membranes. Membranes were blocked in 5% milk or 3% BSA in TBS
991 supplemented with 0.1% Tween-20 (TBS-T) respectively. Membranes were incubated with
992 primary antibodies overnight at 4 °C in blocking buffer, washed three times with TBS-T, incubated
993 with secondary HRP-conjugated antibodies (1:10,000) for 1 h at room temperature, washed again
994 with TBS-T and immediately analyzed by enhanced chemiluminescence.

995

996 **Streptavidin pulldown and sample processing for mass spectrometry**

997 After respective treatment, cells were washed 2 times with ice-cold DPBS, scraped in PBS and
998 pellets either processed immediately or stored at -80°C. Cells were lysed in RIPA buffer for 30
999 min on ice. After clearance by centrifugation at 20,000 × g for 10 min at 4 °C, protein
1000 concentrations were adjusted using BCA assay. Cleared and adjusted supernatants were
1001 incubated overnight on an overhead rotator with preequilibrated streptavidin agarose (Sigma).
1002 Next day, beads were washed 2 times with RIPA buffer, 4 times with freshly prepared 3 M Urea
1003 buffer (Urea in 50 mM ammonium bicarbonate) and suspended in a defined volume of 3 M Urea
1004 buffer. Samples were reduced with 5 mM TCEP (Sigma) at 55 °C for 30 min, alkylated with 10
1005 mM IAA (Sigma) at room temperature for 20 min and quenched with 20 mM DTT (Sigma).
1006 Samples were washed two times with freshly prepared 2 M Urea buffer (Urea in 50 mM
1007 ammonium bicarbonate), suspended in 50 µl of 2 M Urea buffer and digested with 1 µg trypsin
1008 per sample at 37 °C overnight. Peptides were collected by pooling the supernatant with two 50 µl
1009 2 M Urea buffer washes, immediately acidified with 1% trifluoroacetic acid and concentrated by

1010 vacuum centrifugation. Digested peptides were desalted on custom-made C18 stage tips and
1011 reconstituted in 0.1% formic acid.
1012
1013 **MS data collection and analysis**
1014 Peptides were separated using an Easy-nLC1200 liquid chromatograph (Thermo Scientific)
1015 followed by peptide detection on a Q Exactive HF mass spectrometer (Thermo Scientific).
1016 Samples were separated on a 75 µm× 15 cm custom-made fused silica capillary packed with
1017 C18AQ resin (Reprosil-PUR 120, 1.9 µm, Dr. Maisch) with a 35 min acetonitrile gradient in 0.1%
1018 formic acid at a flow rate of 400 nl/min (5–38% ACN gradient for 23 min, 38–60% ACN gradient
1019 for 3 min, 60–95% ACN gradient for 2 min). Peptides were ionized using a Nanospray Flex Ion
1020 Source (Thermo Scientific). Peptides were identified in fullMS / ddMS² (Top15) mode, dynamic
1021 exclusion was enabled for 20 s and identifications with an unassigned charge or charges of one
1022 or >8 were rejected. MS1 resolution was set to 60,000 with a scan range of 300–1650 m/z, MS2
1023 resolution to 15,000. Data collection was controlled by Tune/Xcalibur (Thermo Scientific). Raw
1024 data were analyzed using MaxQuant's (version 1.6.0.1) Andromeda search engine in reversed
1025 decoy mode based on a human reference proteome (Uniprot-FASTA, UP000005640,
1026 downloaded June 2023) with an FDR of 0.01 at both peptide and protein levels. Digestion
1027 parameters were set to specific digestion with trypsin with a maximum number of 2 missed
1028 cleavage sites and a minimum peptide length of 7. Oxidation of methionine and amino-terminal
1029 acetylation were set as variable and carbamidomethylation of cysteine as fixed modifications. The
1030 tolerance window was set to 20 ppm (first search) and to 4.5 ppm (main search). Label-free
1031 quantification was set to a minimum ratio count of 2, re-quantification and match-between runs
1032 was selected and at least 4 biological replicates per condition were analyzed. Resulting protein
1033 group files were processed using Perseus (version 1.6.14.0). Briefly, common contaminants,
1034 reverse and site-specific identifications as well as proteins identified with a peptide count and
1035 MS/MS count <2 were excluded. Protein groups considered for statistical testing had further to
1036 be identified in at least 3 out of 4 replicates in at least one condition. DAVID (version 2021) was
1037 used for functional enrichment analysis.
1038

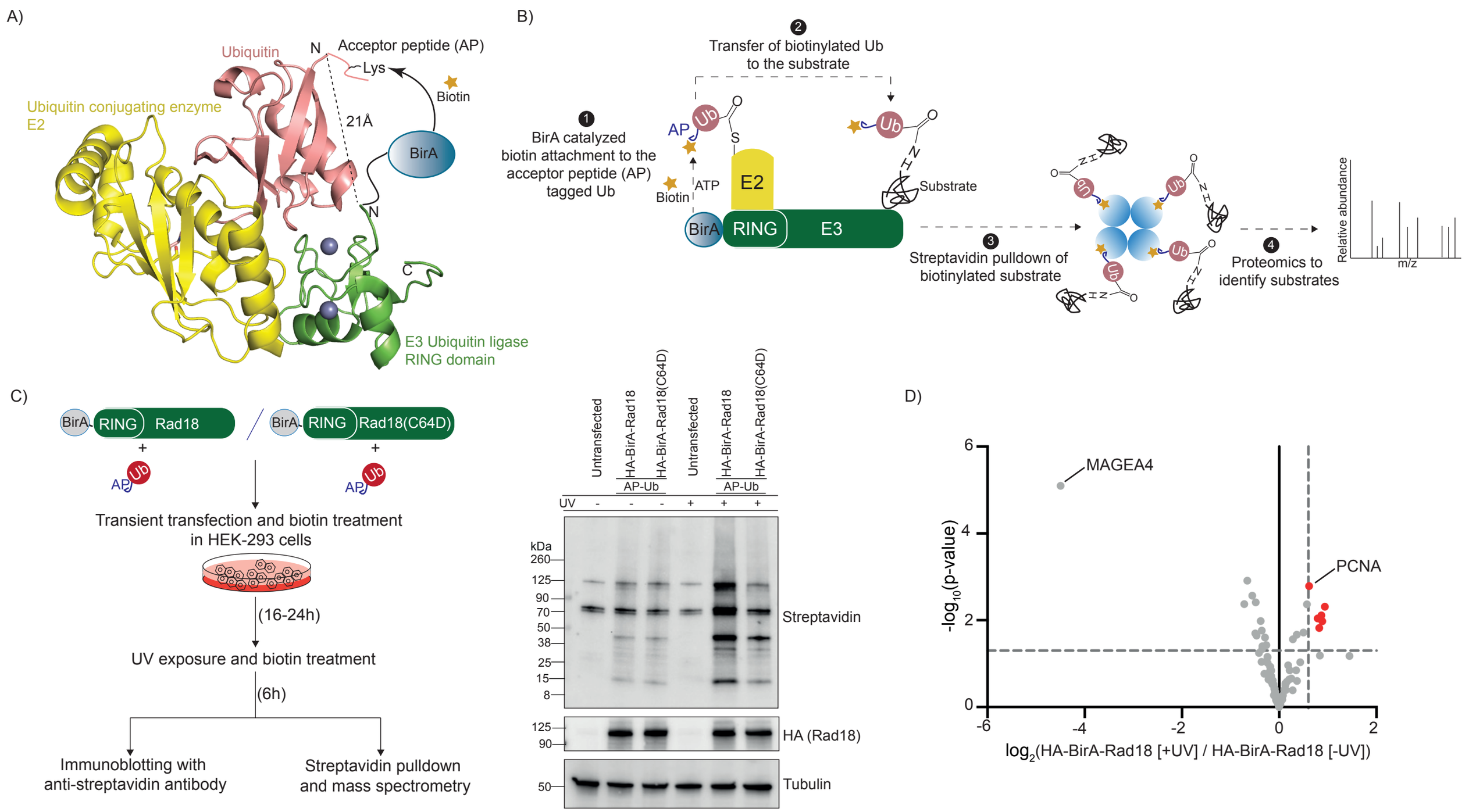
A)
Ubiquitin
N
Acceptor peptide (AP)
Lys
Biotin
Ubiquitin conjugating enzyme E2
21Å
BirA
N
C
E3 Ubiquitin ligase RING domain
B)
2 Transfer of biotinylated Ub to the substrate
1 BirA catalyzed biotin attachment to the acceptor peptide (AP) tagged Ub
AP
Ub
S
ATP
Biotin
E2
BirA
RING
E3
Substrate
3 Streptavidin pulldown of biotinylated substrate
4 Proteomics to identify substrates
Relative abundance
m/z
C)
BirA
RING
Rad18
Rad18(C64D)
+
AP
Ub
Transient transfection and biotin treatment in HEK-293 cells
(16-24h)
UV exposure and biotin treatment
(6h)
Immunoblotting with anti-streptavidin antibody
Streptavidin pulldown and mass spectrometry
Untransfected
HA-BirA-Rad18
HA-BirA-Rad18(C64D)
AP-Ub
UV
kDa
260
125
90
70
50
38
25
15
8
Streptavidin
HA (Rad18)
Tubulin
D)
MAGEA4
PCNA
-log10(p-value)
log2(HA-BirA-Rad18 [+UV] / HA-BirA-Rad18 [-UV])

Figure 1

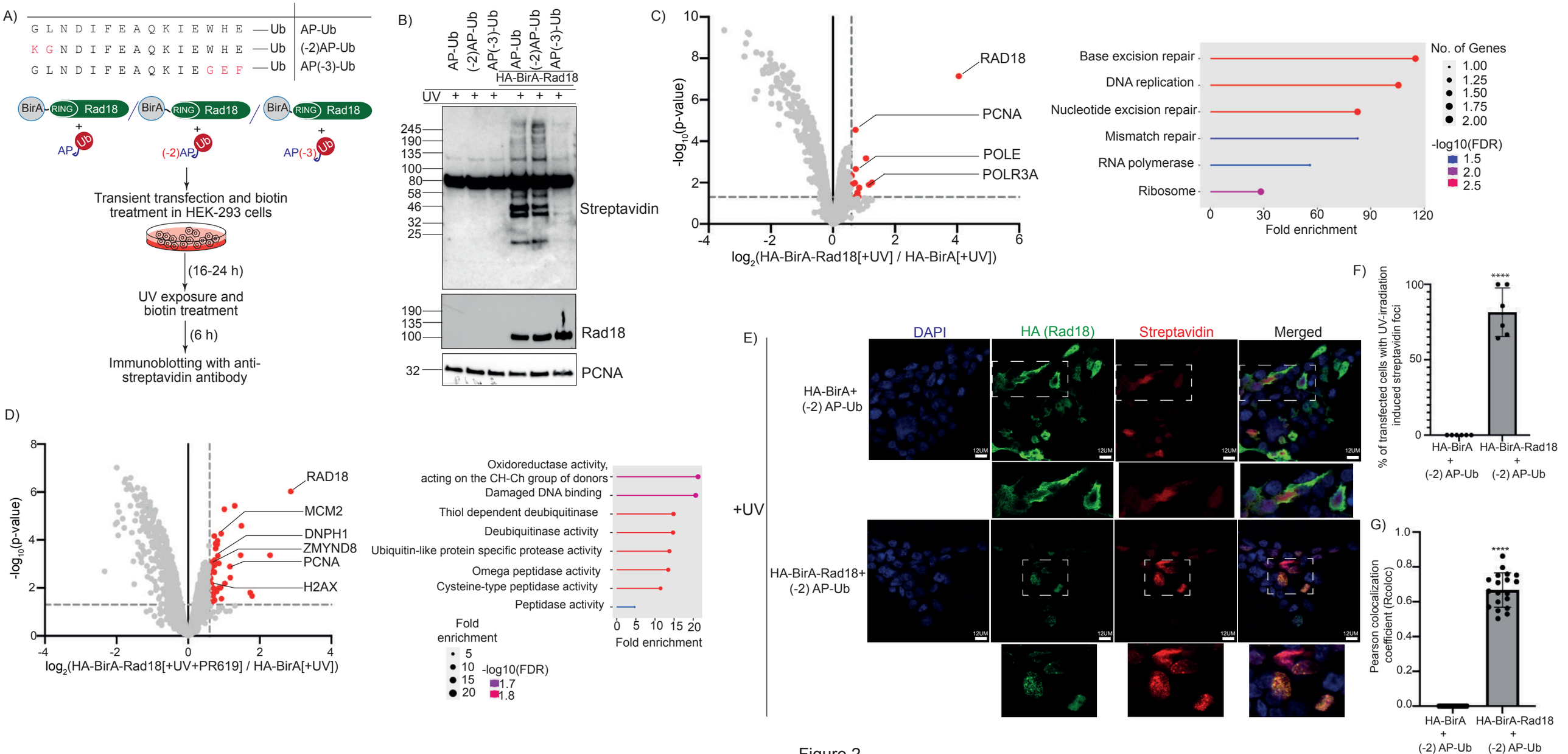
A)
G L N D I F E A Q K I E W H E —Ub AP-Ub
K G N D I F E A Q K I E W H E —Ub (-2)AP-Ub
G L N D I F E A Q K I E G E F —Ub AP(-3)-Ub
BirA RING Rad18 + AP Ub
BirA RING Rad18 + (-2)AP Ub
BirA RING Rad18 + AP(-3) Ub
Transient transfection and biotin treatment in HEK-293 cells
(16-24 h)
UV exposure and biotin treatment
(6 h)
Immunoblotting with anti-streptavidin antibody
B)
AP-Ub
(-2)AP-Ub
AP(-3)-Ub
AP-Ub
(-2)AP-Ub
AP(-3)-Ub
HA-BirA-Rad18
UV + + + + + +
245
190
135
100
80
58
46
32
25
Streptavidin
190
135
100
Rad18
32
PCNA
C)
-log10(p-value)
log2(HA-BirA-Rad18[+UV] / HA-BirA[+UV])
RAD18
PCNA
POLE
POLR3A
Base excision repair
DNA replication
Nucleotide excision repair
Mismatch repair
RNA polymerase
Ribosome
Fold enrichment
No. of Genes
1.00
1.25
1.50
1.75
2.00
-log10(FDR)
1.5
2.0
2.5
D)
-log10(p-value)
log2(HA-BirA-Rad18[+UV+PR619] / HA-BirA[+UV])
RAD18
MCM2
DNPH1
ZMYND8
PCNA
H2AX
Oxidoreductase activity, acting on the CH-Ch group of donors
Damaged DNA binding
Thiol dependent deubiquitinase
Deubiquitinase activity
Ubiquitin-like protein specific protease activity
Omega peptidase activity
Cysteine-type peptidase activity
Peptidase activity
Fold enrichment
Fold enrichment
5
10
15
20
-log10(FDR)
1.7
1.8
E)
DAPI
HA (Rad18)
Streptavidin
Merged
HA-BirA+ (-2) AP-Ub
+UV
HA-BirA-Rad18+ (-2) AP-Ub
12UM
F)
% of transfected cells with UV-irradiation induced streptavidin foci
****
HA-BirA + (-2) AP-Ub
HA-BirA-Rad18 + (-2) AP-Ub
G)
Pearson colocalization coefficient (Rcoloc)
****
HA-BirA + (-2) AP-Ub
HA-BirA-Rad18 + (-2) AP-Ub

Figure 2

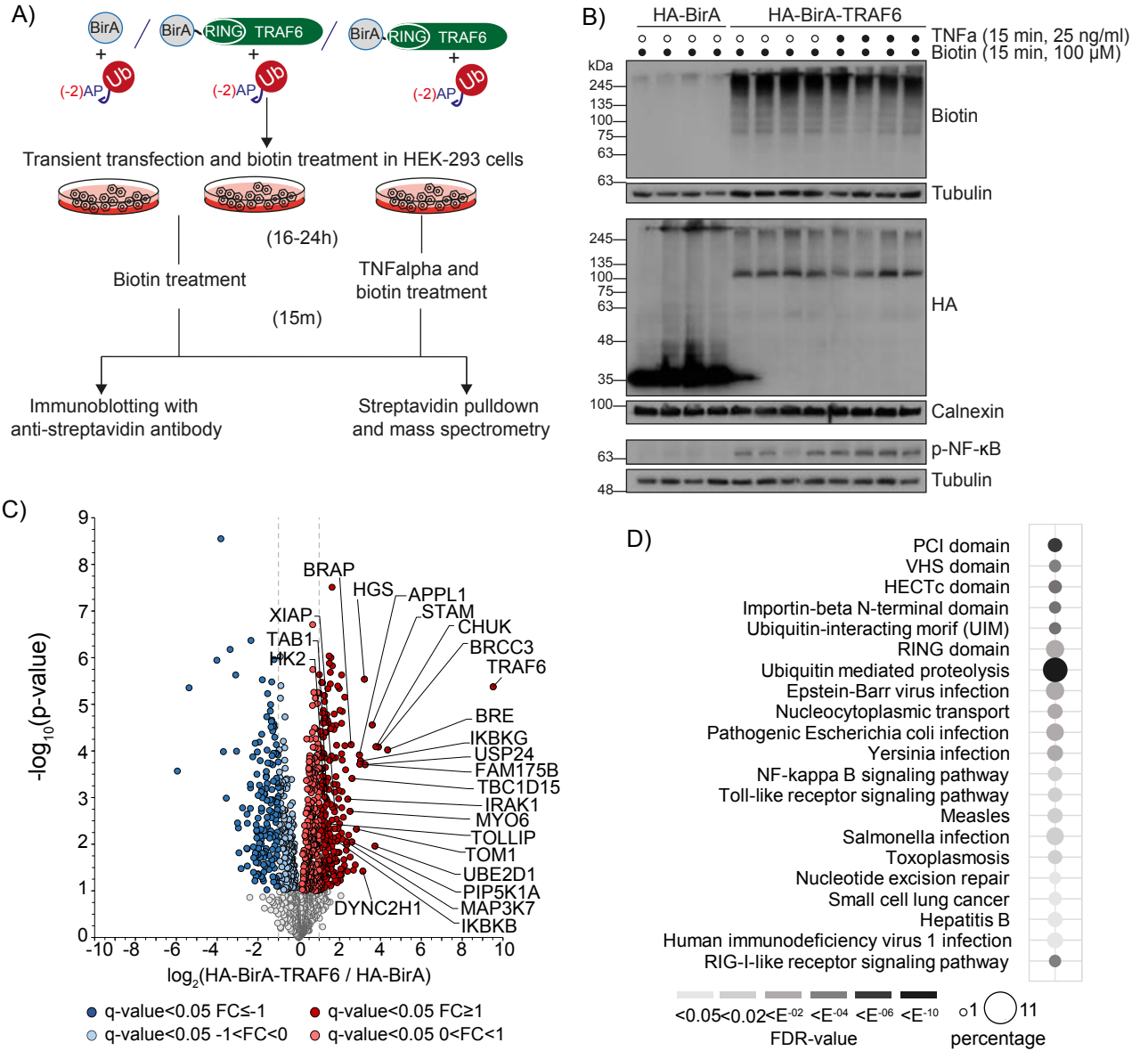
A)
BirA
BirA
RING
TRAF6
BirA
RING
TRAF6
+
Ub
(-2)AP
Transient transfection and biotin treatment in HEK-293 cells
(16-24h)
Biotin treatment
TNFalpha and biotin treatment
(15m)
Immunoblotting with anti-streptavidin antibody
Streptavidin pulldown and mass spectrometry
B)
HA-BirA
HA-BirA-TRAF6
TNFa (15 min, 25 ng/ml)
Biotin (15 min, 100 μM)
kDa
245
135
100
75
63
48
35
Biotin
Tubulin
HA
Calnexin
p-NF-κB
C)
-log10(p-value)
log2(HA-BirA-TRAF6 / HA-BirA)
BRAP
HGS
APPL1
STAM
CHUK
BRCC3
TRAF6
XIAP
TAB1
IRK2
BRE
IKBKG
USP24
FAM175B
TBC1D15
IRAK1
MYO6
TOLLIP
TOM1
UBE2D1
PIP5K1A
MAP3K7
IKBKB
DYNC2H1
q-value<0.05 FC≤-1
q-value<0.05 FC≥1
q-value<0.05 -1<FC<0
q-value<0.05 0<FC<1
D)
PCI domain
VHS domain
HECTc domain
Importin-beta N-terminal domain
Ubiquitin-interacting morif (UIM)
RING domain
Ubiquitin mediated proteolysis
Epstein-Barr virus infection
Nucleocytoplasmic transport
Pathogenic Escherichia coli infection
Yersinia infection
NF-kappa B signaling pathway
Toll-like receptor signaling pathway
Measles
Salmonella infection
Toxoplasmosis
Nucleotide excision repair
Small cell lung cancer
Hepatitis B
Human immunodeficiency virus 1 infection
RIG-I-like receptor signaling pathway
<0.05<0.02<E-02 <E-04 <E-06 <E-10
FDR-value
1
11
percentage

Figure 3

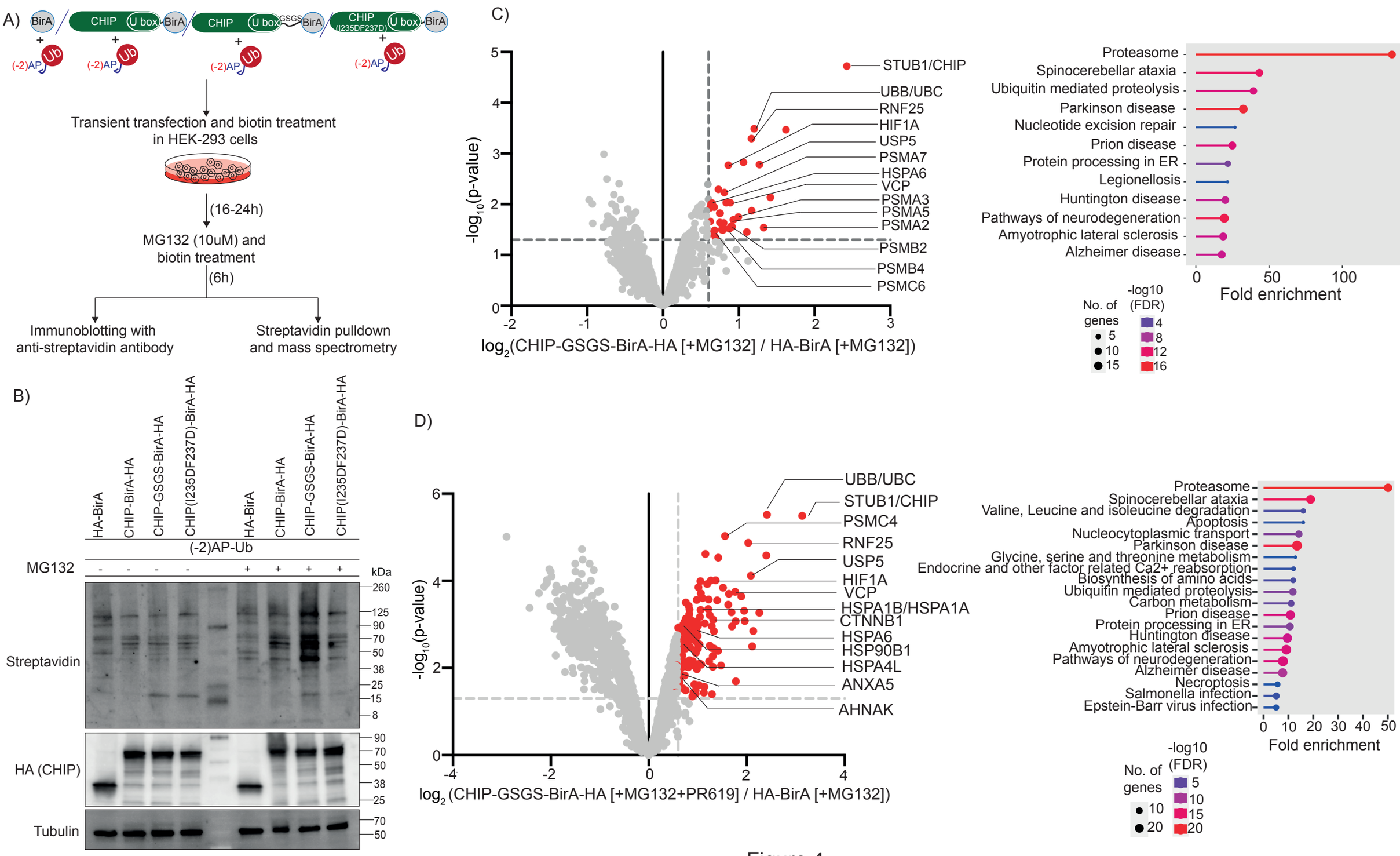
A)
BirA
CHIP
U box
BirA
GSGS
CHIP (I235DF237D)
(-2)AP
Ub
Transient transfection and biotin treatment in HEK-293 cells
(16-24h)
MG132 (10uM) and biotin treatment
(6h)
Immunoblotting with anti-streptavidin antibody
Streptavidin pulldown and mass spectrometry
B)
HA-BirA
CHIP-BirA-HA
CHIP-GSGS-BirA-HA
CHIP(I235DF237D)-BirA-HA
(-2)AP-Ub
MG132
kDa
Streptavidin
HA (CHIP)
Tubulin
C)
STUB1/CHIP
UBB/UBC
RNF25
HIF1A
USP5
PSMA7
HSPA6
VCP
PSMA3
PSMA5
PSMA2
PSMB2
PSMB4
PSMC6
-log10(p-value)
log2(CHIP-GSGS-BirA-HA [+MG132] / HA-BirA [+MG132])
Proteasome
Spinocerebellar ataxia
Ubiquitin mediated proteolysis
Parkinson disease
Nucleotide excision repair
Prion disease
Protein processing in ER
Legionellosis
Huntington disease
Pathways of neurodegeneration
Amyotrophic lateral sclerosis
Alzheimer disease
Fold enrichment
No. of genes
-log10 (FDR)
D)
UBB/UBC
STUB1/CHIP
PSMC4
RNF25
USP5
HIF1A
VCP
HSPA1B/HSPA1A
CTNNB1
HSPA6
HSP90B1
HSPA4L
ANXA5
AHNAK
log2 (CHIP-GSGS-BirA-HA [+MG132+PR619] / HA-BirA [+MG132])
Valine, Leucine and isoleucine degradation
Apoptosis
Nucleocytoplasmic transport
Glycine, serine and threonine metabolism
Endocrine and other factor related Ca2+ reabsorption
Biosynthesis of amino acids
Carbon metabolism
Necroptosis
Salmonella infection
Epstein-Barr virus infection

Figure 4

Ub-POD parameters/recommendations

1) Tagging BirA

> For RING and Ubox ligases tag BirA at the catalytic end
> For HECT and RBR ligases tag BirA at the C terminus

2) Inducers

> Overexpression of the candidate ligase
> For ligases which carry out degradative ubiquitination, use proteasome inhibitors
> Use ligase-specific inducers such as UV exposure for Rad18 where applicable.
> Use DUB inhibitor, PR619 for preventing Ub recycling and preserving the substrate ubiquitination
> Use of specific cell lines where the ligase is known to be active

3) Controls for the proteomics

> HA-BirA can be used as a control for any E3 ligase.
> E3-E2 interaction interface mutant for RING and U-box/ and catalytic cysteine to alanine for HECT and RBR ligases
> No inducer treatment can also act as a control

4) Linker between BirA and the ligase

> Structural models of E3-E2~Ub can be analyzed to assess whether a linker is needed
> Generation of constructs with and without a GSGS linker are recommended for initial trials
> Longer linkers may be needed for HECT ligases
> Linker length needs to optimized for adapting Ub-POD to UBLs

5) Different biotin treatment regimes

> Exposing cells to Biotin throughout the Ub-POD experiment is recommended
> Shorter biotin exposure regimes (adding biotin only during treatment with the inducer) could be tested

Figure 5